DOCUMENT

document title/ titre du document

ENVISAT CYCLIC ALTIMETRIC REPORT

CYCLE 28 from 21-06-2004 to 26-07-2004

Quality Assessment Report

prepared by/*préparé par*	EOP-GOQ and PCF team
reference/*réference*	ENVI-GSOP-EOPG-03-0011
issue/*édition*	1
revision/*révision*	0
date of issue/*date d'édition*	28 September 2004
status/*état*	
Document type/*type de document*	Technical Note
Distribution/*distribution*	

European Space Agency
Agence spatiale européenne

TABLE OF CONTENTS

1 INTRODUCTION

This documents aims at reporting on the performances of the EnviSat Radar Altimeter, Microwave Radiometer and DORIS sensors, on the data quality of the corresponding Fast Delivery products (RA2_FGD_2P) as well as on the main events occurred during cycle 28.

This reports covers the period from the 21st of June and the 26th of July 2004.

2 DISTRIBUTION LIST

This report is available in PDF format at the internet address http://earth.esa.int/pcs/envisat

3 ACRONYMS

AGC	Automatic Gain Control
DORIS	Doppler Orbitography and Radiopositioning Integrated by Satellite
DSR	Data Set Record
EPC	Electronic Power Converter
ERS	European Remote Sensing satellite
ESRIN	European Space Research Institute
ESOC	European Space Operations Centre
FD	Fast Delivery products
GS	Ground Segment
GTS	Global Telecommunication System
HTL	Height Tracking Loop
ICU	Instrument Control Unit
IECF	Instrument Engineering Calibration Facility
IF	Intermediate Frequency
IE	Individual Echoes
IPF	Instrument Processing Facility
LUT	Look Up Table
MCMD	MacroCommand
MPH	Main Product Header
MSS	Mean Sea Surface
MWR	MicroWave Radiometer
MPS	Mission Planning System
OBT	On-Board Time
OCM	Orbit Control Mode/Manoeuvres
PCS	ERS Products Control Service
PCF	EnviSat Product Control Facility
PDHS-E	ESRIN Processing and Data Handling Station
PDHS-K	Kiruna Processing and Data Handling Station
PLSOL	Payload Switch-Off Line

PMC	Payload Main Computer
PTR	Point Target Response
RA-2	EnviSat Radar Altimeter bi-frequency
RSL	Resolution Selection Logic
SAD	Static Auxiliary Files
SBT	Satellite Binary Time
SEU	Single Event
SFCM	Stellar Fine Control Mode
SPH	Specific Product header
SPSA	Signal Processing Sub-Assembly
SYSM	Stellar Yaw Steering Mode
S/W	Software
TM	Telemetry
TRP	Transponder
TWT	Traveling Wave Tube
UTC	Coordinated Universal Time
YSM	Yaw Stellar Mode

4 REFERENCE DOCUMENTS

[R – 1] F-PAC MONTHLY REPORT, SALP-RP-M-OP-15306-CN, July 2004
[R – 2] ENVISAT Microwave Radiometer Assessment Report Cycle 028, CLS.DOS/04.182, http://earth.esa.int/pcs/envisat/mwr/reports/
[R – 3] Envisat RA-2 IF Mask weird behavior: Investigation Report
[R – 4] Instrument Performance Evaluation and Analysis Summary, PO-TR-ALS-RA-0042
[R – 5] Instrument Corrections Applied on RA-2 Level 1b products, Paper presented at the ENVISAT Calibration Review in September 2002
[R – 6] ENVISAT Phase E Cal/Val Acquisition Plan, ENVI-SPPA-EOPG-TN-03-0008
[R – 7] RA-2 S-Band Anomaly Investigation, PO-TN-ESA-RA-1331, http://earth.esa.int/pcs/envisat/ra2/articles/
[R – 8] RA-2 Performance Results, Paper presented at the ENVISAT Calibration Review in September 2002
[R – 9] ECMWF Report on ENVISAT RA- 2 for July 2004, Report on ENVISAT Radar Altimeter - 2 (RA- 2), Wind/ Wave Product with Height Information (RA2_ WWV_ 2P), http://earth.esa.int/pcs/envisat/ra2/reports/ecmwf/
[R – 10] Envisat GDR Quality Assessment Report, SALP-RP-P2-EX-21121-CLS015
[R – 11] Envisat RA-2 Range Instrumental correction: USO clock period variations and associated auxiliary file, ENVI-GSEG-EOPG-TN-03-0009
[R – 12] Defining a Rain flag for the Envisat altimeter, G. Quartly, study presented to the final CCVT plenary meeting, http://earth.esa.int/pcs/envisat/ra2/articles/
[R – 13] ENVISAT Weekly Mission Operations Reports # 107-111, ENVI-ESOC-OPS-RP-1011-TOS-OF
[R – 14] Envisat validation and cross calibration activities during the verification phase. Synthesis Report ESTEC contract No. 16243/02/NL/FF WP6, http://earth.esa.int/pcs/envisat/ra2/articles/

[R – 15] ENVISAT-1 Products Specifications - Vol. 14: RA-2 Products Specifications, PO-RS-MDA-GS-2009, Iss 3, Rev. K, 24/05/2004
[R – 16] Algorithm for Flag identification and waveforms reconstruction of RA-2 data affected by “S-Band anomaly”, ENVI-GSEG-TN-04-0004, Issue 1.4

5 GENERAL QUALITY ASSESSMENT

5.1 *Instruments status*

The RA-2 instrument, during this cycle underwent one instrument anomaly as given in par. 6.1.

The two known causes of random on-board anomalies are still present. In particular we refer to the so-called S-Band anomaly and the IF mask weird behavior described respectively in [R – 7] and [R – 3]. Only the S-Band anomaly partially affects a low number of Envisat data products as given in par. 7.1.7.

MWR sensor assessment report: refer to [R – 2].

DORIS sensor assessment report: refer to [R – 1].

5.2 *Cycle quality*

The summary of the RA-2 data products availability for this cycle is given in Table 1.

Start orbit	Stop orbit	Time instrum. unavailability	Time L0 gaps	Time L1b gaps	Time L2 (FGD) gaps	% instrum. avail.	% L0 avail.	% L1b avail.	% L2 (FGD) avail.
12079	12179,2	1012,026	545,152	545,152	6439,474	99,83267	99,74253	99,74253	98,76794
12179,2	12279,4	1077,693	4830,384	4828,384	10721,31	99,82181	99,02314	99,02347	98,04911
12279,4	12379,6	1070,937	4172,389	4169,134	4179,628	99,82293	99,13305	99,13359	99,13185
12379,6	12479,8	23210,01	1145,031	7000,059	13090,8	96,16237	95,97305	95,00496	93,99789
12479,8	12580	1089,387	2900,998	7213,316	9030,37	99,81988	99,34021	98,6272	98,32676

Table 1: RA-2 L0, L1b and L2 FGD Data products availability summary for cycle 28

5.3 *Orbit quality*

During cycle 28 the orbit was maintained within the +/- 1km to the reference ground track.
On the 30-June-2004, a 1-burn SFCM orbit maintenance manoeuvre was executed as planned. The following table summarizes the SFCM observed performance:

	Burn Start Time	Nominal Delta-V	Calibrated Delta-V	Mode
First burn	2004/06/30-09:08:00	0.0132 m/sec	0.0130 m/sec	SFCM

On the 21-June-2004 a Platform anomaly was triggered at 07:05:33 with a transition to Yaw Stellar Mode. The anomaly is linked to the appearance of a very bright object across the Star Tracker field that caused its software to stop. Recovery was successfully performed leading to a transition back to the nominal operating mode (SYSM) on 22-June-2004 at 11:50:19.

5.4 Ground Segment Processing Chain Status

5.4.1 IPF PROCESSING CHAIN

July 16, 2004: Installed IPF version 4.58. This is equivalent to the previous version for what regards all the algorithms and auxiliary files, only a new parameter has been added in the SPH that is the pass number which, for NRT data is nominally set to 0. This was done in order to be compliant with the off-line products version that indeed includes the pass number.

Previous IPF version V4.57 was operational at the Envisat PDHS-K and PDHS-E since April 29th and 28th 2004 respectively.

5.4.2 F-PAC PROCESSING CHAIN

Current version of CMA is V6.3 operational since Apr. 29, 2004.

F-PAC CMA anomalies: anomalies are detailed in the F-PAC Monthly Report [R - 1].

5.4.3 AUXILIARY DATA FILE

Hereafter all the Auxiliary files used actually used by the IPF ground processing are listed:

```
RA2_CHD_AXVIEC20030402_094243_20030407_000000_20200101_000000
RA2_CON_AXVIEC20020606_164228_20020101_000000_20200101_000000
RA2_CST_AXVIEC20020621_135858_20020101_000000_20200101_000000
RA2_DIP_AXVIEC20020122_134206_20020101_000000_20200101_000000
RA2_GEO_AXVIEC20020314_093428_20020101_000000_20200101_000000
RA2_ICT_AXVIEC20031208_143628_20020101_000000_20200101_000000
RA2_IFA_AXVIEC20020313_174755_20020101_000000_20200101_000000
RA2_IFB_AXVIEC20020313_174959_20020101_000000_20200101_000000
RA2_IFF_AXVIEC20031208_151817_20030602_215929_20100101_000000
RA2_IOC_AXVIEC20020122_141121_20020101_000000_20200101_000000
RA2_MET_AXVIEC20020204_073357_20020101_000000_20200101_000000
RA2_MSS_AXVIEC20031208_145545_20020101_000000_20200101_000000
RA2_OT1_AXVIEC20040120_082051_20020101_000000_20200101_000000
RA2_OT2_AXVIEC20031208_150159_20020101_000000_20200101_000000
RA2_SET_AXVIEC20020122_150917_20020101_000000_20200101_000000
RA2_SL1_AXVIEC20030131_100228_20020101_000000_20200101_000000
RA2_SL2_AXVIEC20030131_101757_20020101_000000_20200101_000000
RA2_SOI_AXVIEC20031208_150608_20020101_000000_20200101_000000
```

```
RA2_SSB_AXVIEC20031208_150749_20020101_000000_20200101_000000
RA2_TLD_AXVIEC20031208_151137_20020101_000000_20200101_000000
RA2_USO_AXVIEC20020122_162920_20020101_000000_20200101_000000
```

The RA2_POL_AX, the RA2_SOL_AX and the RA2_PLA_AX have been regularly updated every week without problems.

The RA-2 Auxiliary Data Files (ADF) are accessible from the Envisat Web pages under http://envisat.esa.int/services/tools_table.html.

5.4.4 PLANNED UPGRADES

Evolution of the IPF Level 1B and Level 2 processing chain is currently planned. The next IPF version release shall nominally contain the following:

1. USO instrumental correction within the RA-2 L1b processor.
2. New MWR Side Lobes correction algorithm within MWR L1b processor
3. Correction of the mispointing evaluation algorithm within the RA-2 L2 processor
4. Inclusion of the loading tide for the GOT2000.2 model.
5. Addition of the peakiness fields in Ku and S band to the RA-2 and MWR FD/I/MAR meteorological products
6. Inclusion of the square of the significant wave height in Ku and S band
7. Inclusion of an S-band anomaly flag, see [R – 16]
8. Upgrade of the Level 1B and Level 2 processing for DORIS NRT orbital information computation.

Evolutions 3, 5 and 6 shall be reflected too in the F-PAC CMA processing chain.

6 ENVISAT PAYLOAD STATUS

6.1 Altimeter Events

The Radar Altimeter 2, during cycle 28, was unavailable once, in the following time period:
Start: 18 Jul 2004 13:47:03 Orbit = 12460 RA-2 in Suspend/Reset-Wait due to due to reporting of
Stop: 18 Jul 2004 19:59:00 Orbit = 12464 too many SEUs.

The HSU1 fuse problem (Ref anomaly occurrence during cycle 22) is still present. This problem does not affect nominal operations since the RA-2 instrument is heated by the nearby hardware.

The cause of the problem is still unknown. The heater fuses as well as the hardware used to report on the status of the fuses are presently under examination.

6.1.1 RA-2 INSTRUMENT PLANNING

The RA-2 instrument planning was performed as follows:

- IF Calibration Mode according the nominal operational acquisition scheme: 100 seconds of data per day over Himalayan region.
- Preset Loop Output mode for GAVDOS Range transponders, located in Creta.
- Preset Loop Output acquisition over ESA transponders, located near Rome; for both ascending and descending passes.
- Individual Echoes background planning: buffering of 20 Data block of individual Echoes and transmission of the in the following 160 Data Blocks. This repeated continuously.

Hereafter the map is reported showing the acquisition sites for both the Range and Sigma_0 transponders.

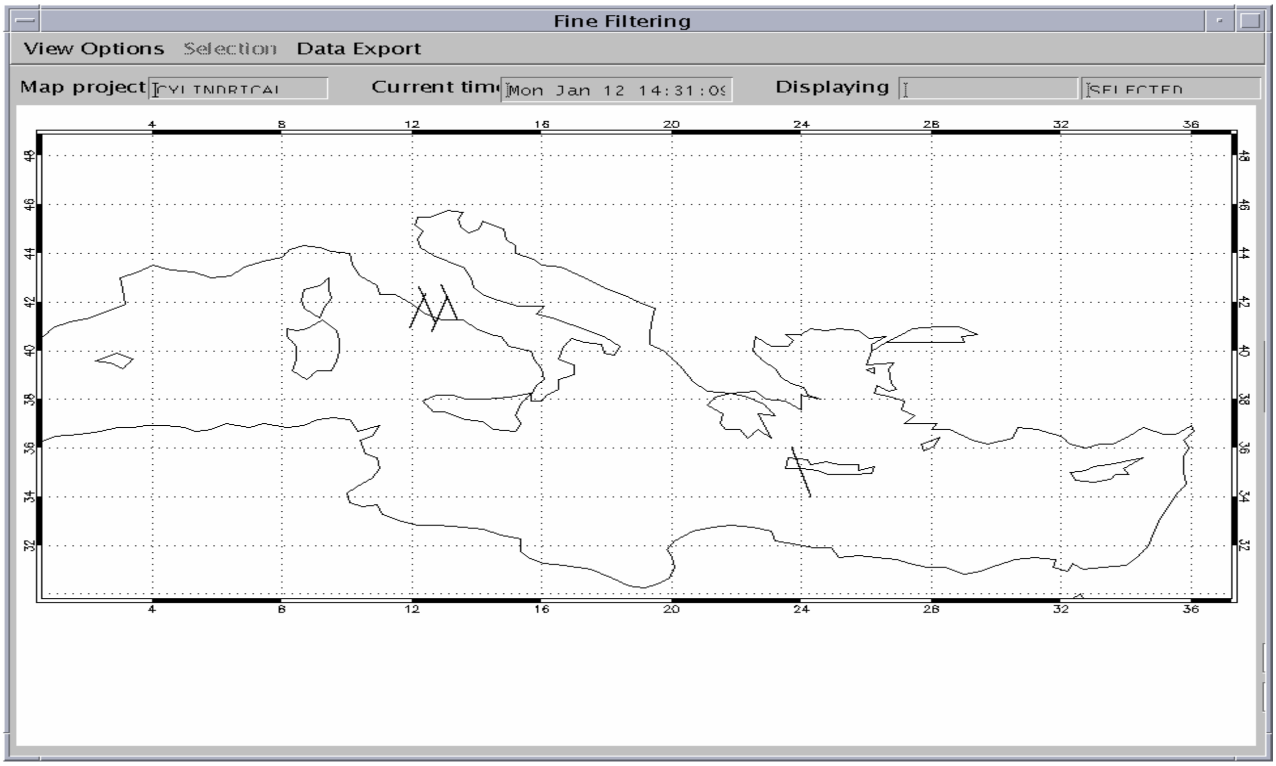

Figure 1: Transponder Acquisition sites for cycle 28

6.2 MWR Events

The MWR, during cycle 28 was never unavailable.

6.3 DORIS Events

The DORIS during cycle 28 was never unavailable.

Starting from June the 14th 2004 the DORIS USO was switched to the redundancy component and it is now working correctly.

7 INSTRUMENT PERFORMANCES

7.1 RA-2 Performances

7.1.1 IF FILTER MASK

In Figure 2 all valid IF masks retrieved by averaging the 100 seconds of data acquired daily during cycle 28 are plotted in the left panel. The on-ground measured IF mask (ref [R – 4]) is also plotted in that panel with a red solid line. In the right panel the difference of each of the calculated IF masks with respect to the on-ground measured one is reported. During cycle 28 the number of valid IF masks has been of 7, representing about the 20% of the total available IF masks. Only valid IF masks are used to generate the final IF mask used in the Level 1B ground processing; the method used for editing the data is based on the comparison between each of the single IF masks and the reference one (on-ground).

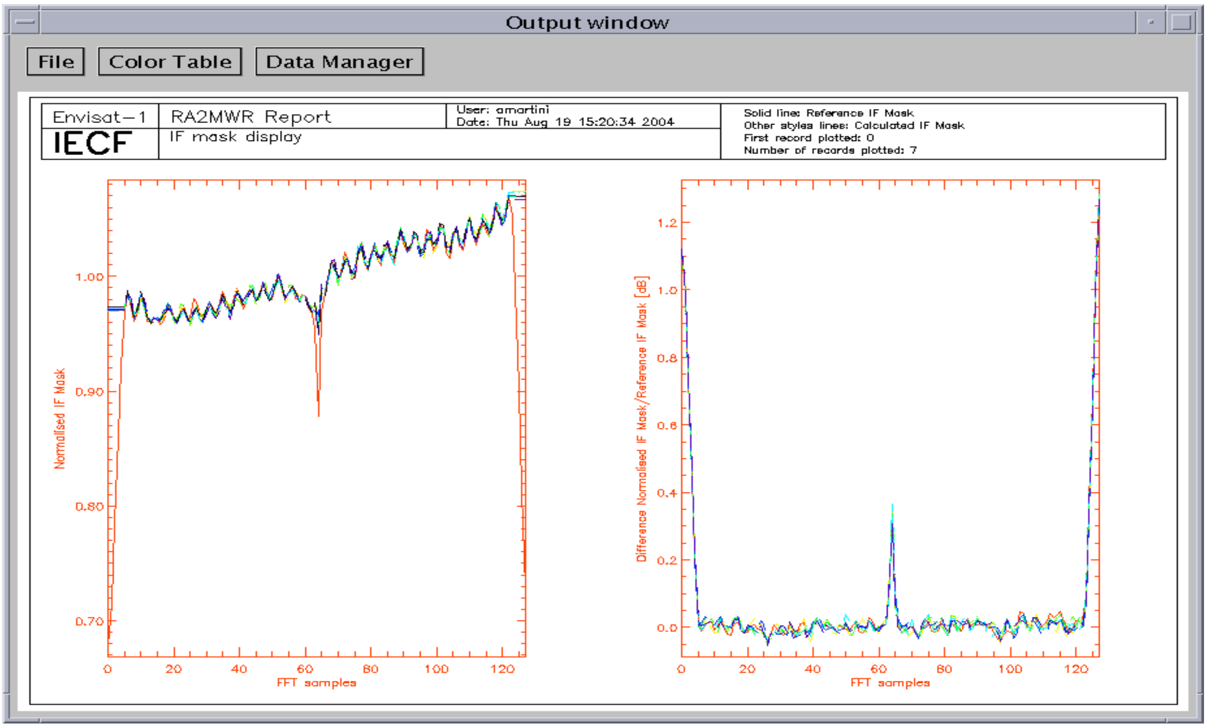

Figure 2: Valid IF masks retrieved daily during cycle 28 plotted together with the on-ground reference.

7.1.2 USO

In Figure 3 the USO clock period trend retrieved for cycle 28 is reported. In order to make the variability visible, the difference of the actual USO clock period with respect to the nominal one has been plotted, in the upper panel. In the lower panel the Range error due to the USO clock variability has been reported taking a satellite altitude of 800 Km as a nominal value.

Currently the nominal USO clock period (12500 ps) is used within the processing, this means that the data are not corrected for the bias and the drift correlated to the actual USO clock period.

A particular investigation has been performed regarding the USO clock trend and the associated auxiliary file; this is described in [R – 11]. The conclusion can be summarized as follows: the precision of 1ps available in the current USO auxiliary file is not enough to appreciate its trend and it is too rough for any altimetric application. A suitable resolution is considered to be of 10^{-6} ps. This problem will be corrected with the following upgrade of the IPF as described in par. 5.4.4.

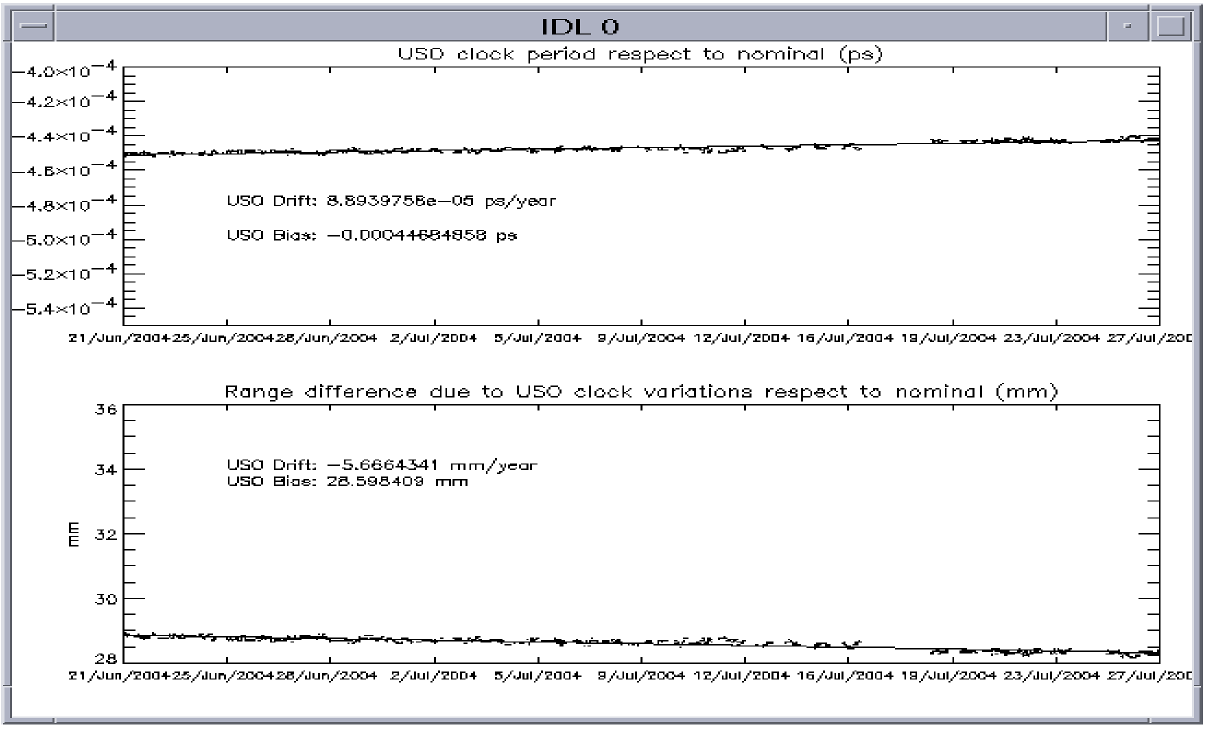

Figure 3: USO clock period for cycle 28

7.1.3 TRACKING CAPABILITY

In Figure 4 and Figure 5, the Chirp ID is plotted respectively for ascending and descending passes of cycle 28. The MDSRs acquired with 320MHz bandwidth are plotted in light gray (Chirp ID equal to 0), the ones acquired with 80MHz bandwidth are plotted in violet (Chirp ID equal to 1) and the ones acquired with the 20MH bandwidth are plotted in dark green (Chirp ID equal to 2).

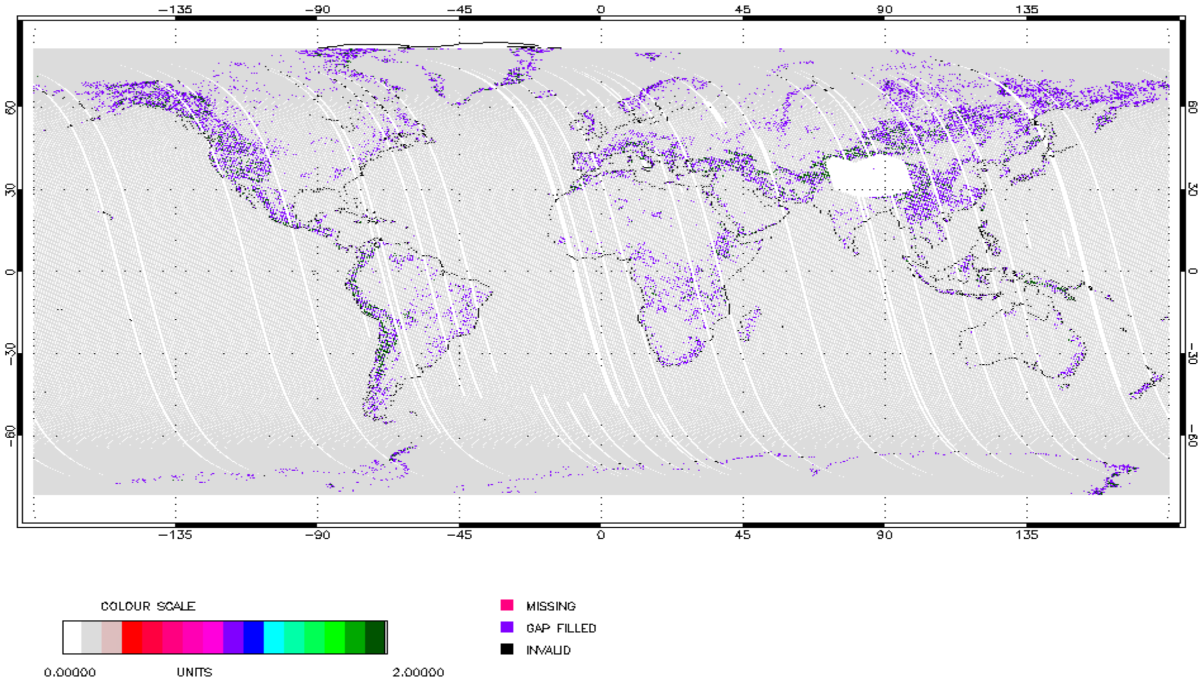

Figure 4: RA-2 Chirp ID for ascending passes during cycle 28

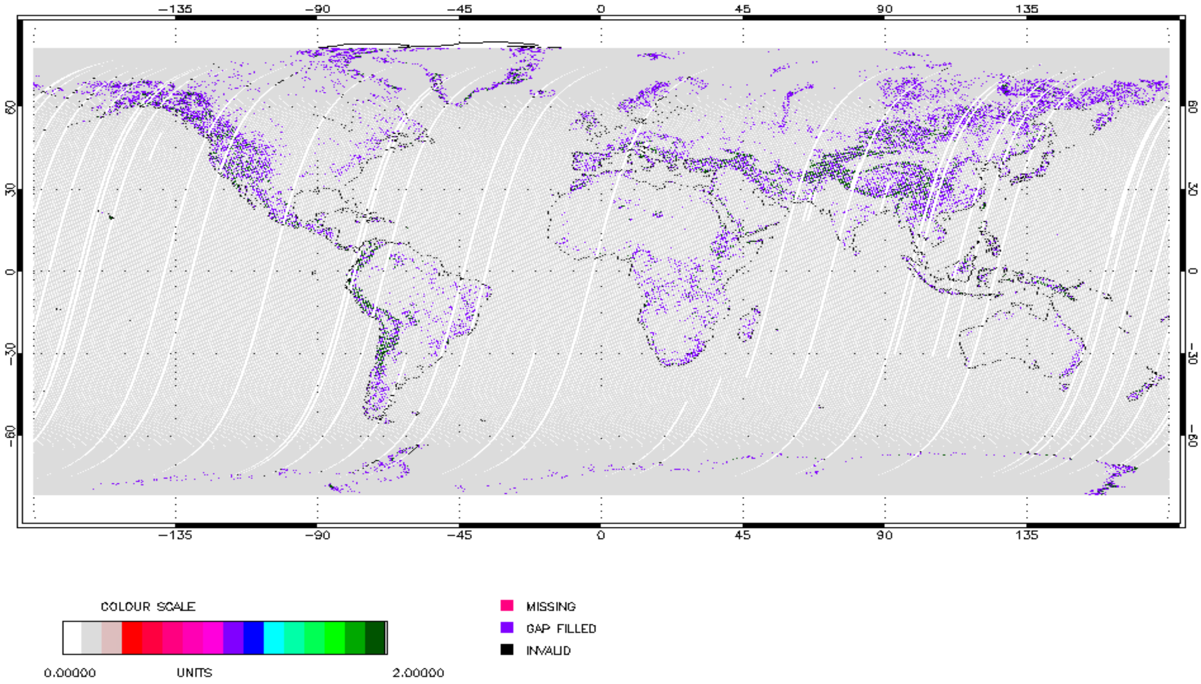

Figure 5: RA-2 Chirp ID for descending passes during cycle 28

The corresponding percentages of acquisition in the different resolutions subdivided by surface type are given in Table 2:

Surface type	320 MHz	80 MHz	20MHz
Open Ocean	99.99%	0.009%	0.001%
Costal Water (ocean depth < 200 m)	98.34%	1.45%	0.21%
Sea Ice	99.19%	0.76%	0.05%
Ice Sheet	96.26%	3.10%	0.64%
Land	81.67%	14.30%	4.03%
All world	95.09%	3.92%	0.99%

Table 2: RA-2 Tracking capability: Chirp ID percentages discriminated by surface type

The figures given for the RA-2 tracking performances during this cycle are very much in line with the ones recorded at the end of the Commissioning Phase and presented in [R – 8]. The slight differences are in part due to the different algorithms used to discriminate the surface types.

The objectives of the Commissioning Phase "RSL and Tracking optimization" are hereafter reported:

320MHz over Ocean > 99%
320 MHz within 15km of Land/Ocean boundary (Costal Water)
320 MHz over Sea Ice > 95%
320/80 MHz Fixed resolution at Ice Sheet Crossovers > 95%
320MHz over Ice Shelves > 95%

7.1.4 SIGMA0 TRANSPONDER

During cycle 28 one Sigma_0 Transponder measurement was performed on the following date:

24-JUN-2004 20:36:27

The other three planned acquisitions were not performed due to a Transponder failure. The problem has already been identified and it will be solved as soon as possible.
The only successful acquisition of this cycle was performed at low resolution because there is still problem that does not allow the instrument to acquire data perfectly centered in the receiving window. The failure of the transponder prevents us to make progress in the investigation of this problem that will start again as soon as the transponder will be repaired.

On the other hand, all the measurements acquired until now have been processed giving the following results:

Orbit	Date	Location/Rel. Track	Coordinates	Resolution	Not Corrected Backscattering Bias [dB]	Wet Tropospheric Correction (one way) [dB]

10389	24-feb-04	Rome/315	41.8472, 12.4819	Low	1,552	0,0606
10511	04-mar-04	Valmontone/437	41.7673, 12.9247	Low	1,542	0,0519
10618	11-mar-04	Fiuggi/43	41.7875, 13.2212	Low	1,447	0,0578
10783	23-mar-04	Maccarese/208	41.8605, 12.2385	Low	1,54	0,0636
10890	30-mar-04	Rome/315	41.8472, 12.4819	Low	1,442	0,0789
11513	13-mag-04	Valmontone/437	41.7673, 12.9247	Low	1,353	0,0672
11620	20-mag-04	Fiuggi/43	41.7875, 13.2212	Low	1,417	0,0719
11892	08-giu-04	Rome/315	41.8472, 12.4819	Low	1,504	0,0772
12014	17-giu-04	Valmontone/437	41.7673, 12.9247	Low	1,448	0,2538
12121	24-giu-04	Fiuggi/43	41.7875, 13.2212	Low	1,576	0,0767
11119	15-apr-04	Fiuggi/43	41.7875, 13.2212	High	0,963	0,0588

Table 3: Absolute backscattering calibration results obtained with Transponder measurements

As it is possible to notice from Table 3 the values obtained at Low resolution are about 0.5 dB higher than the one obtained at High resolution, which is in agreement with the Commissioning Phase Transponder results.

7.1.5 DATATION

A significant part of an eventual error in the RA-2 products datation could be given by the not perfect synchronism between the Satellite Binary Time and the UTC Time due to a drift of the ICU clock period. A correlation between those two times is performed at every Kiruna orbit dump and then extrapolated for the four non-Kiruna orbits. In Figure 6 (upper panel) the differences between the extrapolated UTC values and the corresponding real UTC values measured at the next Kiruna dump, are reported. For the whole cycle they are well under the 20 microseconds warning threshold. In the lower panel the ICU clock step for the same period is shown.

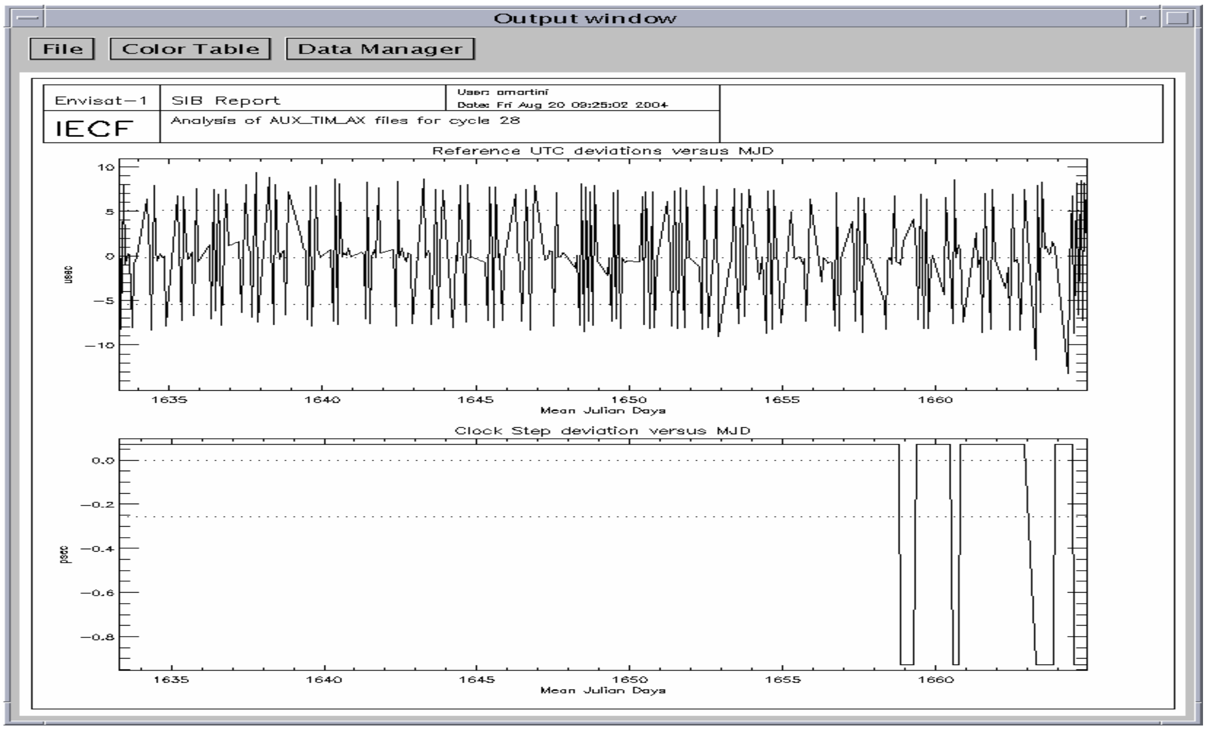

Figure 6: UTC deviations and ICU clock period for cycle 28

7.1.6 MISPOINTING

In Figure 7 the trend of the mispointing squared (averaged every orbit) is reported in deg^2*10e-4 The average mispointing value, as extracted from the RA2_FGD_2P data products, is around 0.027 deg^2, is known to be higher than the one reported at platform level [R – 13]. This is due to a not perfect tuning of the algorithm currently used to retrieve the mispointing value from the RA-2 waveform data. An optimization of this algorithm shall be part of the next Level 2 processors upgrade, planned for end-2004 (ref. 5.4.4).

In particular for this cycle two events of strange mispointing values are visible in the plot; the first one is related to the attitude problems as given in par. 5.3, while the second was in correlation with the occurrence of the instrument anomaly as reported in par. 6.1. The explanation of the anomalous mispointing behavior in correspondence to instrument switch-offs is given in par 7.1.6.

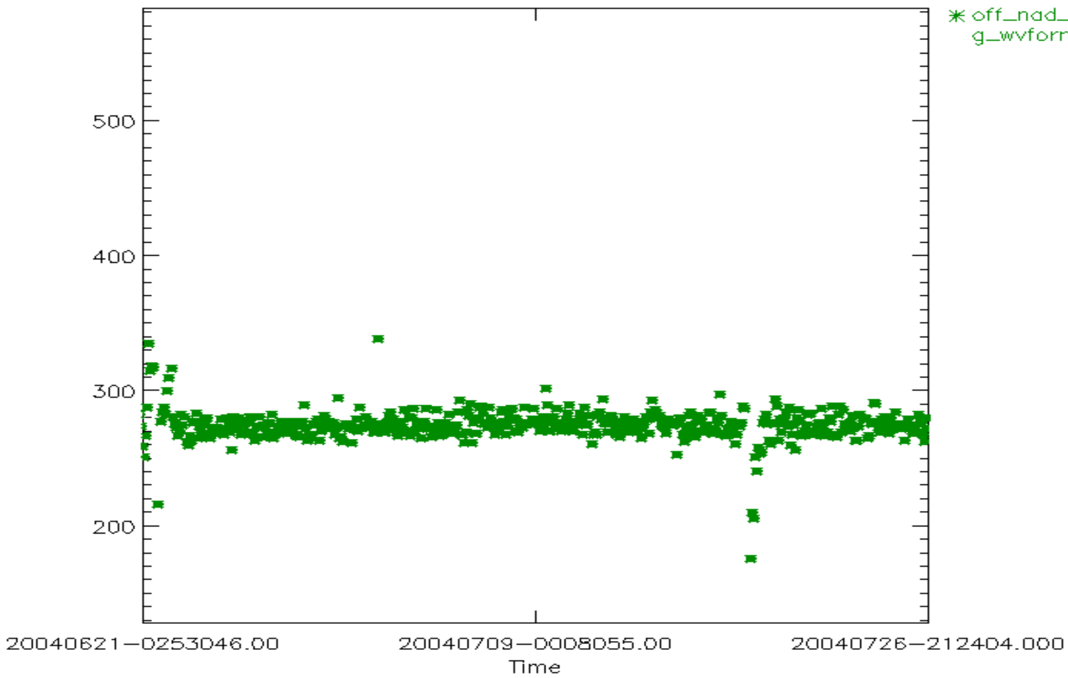

Figure 7: Smoothed mispointing squared trend for cycle 28 (deg^2*10^4)

7.1.7 S-BAND ANOMALY

The so-called "S-Band anomaly" affects the RA-2 data products quality. Hereafter, the table lists the products files affected by the S-band anomaly problem during cycle 28. This corresponds to a total percentage of about 3 % of the acquired data.

Being the method used a statistical one working on ocean data; files containing less than 1000 seconds of data over ocean have not been considered. This choice is supported by the fact that the "S-Band anomaly" is associated to a particular instrumental behavior that cannot appear and disappear within a short time frame. (ref. [R – 7])

File name	Start date	Start time	Stop date	Stop time
RA2_FGD_2PNPDK20040715_080827_000060692028_00336_12414_0285.N1	15-JUL-2004	08:08:27.993522	15-JUL-2004	09:49:37.009611
RA2_FGD_2PNPDK20040715_112910_000059532028_00338_12416_0295.N1	15-JUL-2004	11:29:10.333091	15-JUL-2004	13:08:23.493179
RA2_FGD_2PNPDK20040715_130749_000059422028_00339_12417_0288.N1	15-JUL-2004	13:07:49.014887	15-JUL-2004	14:46:51.034976
RA2_FGD_2PNPDK20040719_110329_000059652028_00395_12473_0330.N1	19-JUL-2004	11:03:29.632033	19-JUL-2004	12:42:55.046124
RA2_FGD_2PNPDK20040719_124221_000059422028_00396_12474_0331.N1	19-JUL-2004	12:42:21.681824	19-JUL-2004	14:21:23.701915
RA2_FGD_2PNPDK20040719_142049_000050632028_00397_12475_0332.N1	19-JUL-2004	14:20:49.223608	19-JUL-2004	15:45:12.297682
RA2_FGD_2PNPDE20040724_035628_000060322028_00462_12540_0340.N1	24-JUL-2004	03:56:28.382987	24-JUL-2004	05:37:00.637073
RA2_FGD_2PNPDE20040724_053625_000061542028_00463_12541_0341.N1	24-JUL-2004	05:36:25.044772	24-JUL-2004	07:18:58.724864
RA2_FGD_2PNPDK20040724_071822_000040082028_00464_12542_0425.N1	24-JUL-2004	07:18:22.018566	24-JUL-2004	08:25:10.134712
RA2_FGD_2PNPDK20040724_082422_000061982028_00465_12543_0426.N1	24-JUL-2004	08:24:22.288415	24-JUL-2004	10:07:40.528491
RA2_FGD_2PNPDK20040724_100704_000059532028_00466_12544_0427.N1	24-JUL-2004	10:07:04.936187	24-JUL-2004	11:46:18.096273
RA2_FGD_2PNPDK20040724_114542_000059772028_00467_12545_0428.N1	24-JUL-2004	11:45:42.503979	24-JUL-2004	13:25:19.058067

RA2_FGD_2PNPDK20040724_132444_000059682028_00468_12546_0429.N1	24-JUL-2004	13:24:44.579775	24-JUL-2004	15:04:12.221865
RA2_FGD_2PNPDK20040724_150335_000050962028_00469_12547_0430.N1	24-JUL-2004	15:03:35.515559	24-JUL-2004	16:28:32.009647

Table 4: List of L2 FGD Files affected by S-Band anomaly during cycle 28

A valuable algorithm to detect the RA-2 DSRs affected by the S-Band anomaly within the L2 products can be found in [R- 12]. Note that the algorithm is only valid for data acquired over open-ocean.

7.2 MWR Performances

For MWR performances please refer to the Reference CLS Cyclic Report of the type of [R – 2].

7.3 DORIS Performances

For DORIS performances refer to the Reference F-PAC Monthly Report of the type of [R - 1].

8 PRODUCT PERFORMANCES

8.1 Availability of data

In Figure 8 and Table 5 the summary of unavailable RA-2 L0 products is given.
It is easy to notice that close to the Himalayan region a small gap in the data is present. This is due to the daily instrument switch-off (Heater 2 mode) performed to prevent the S-Band anomaly to last more than one day when it occurs

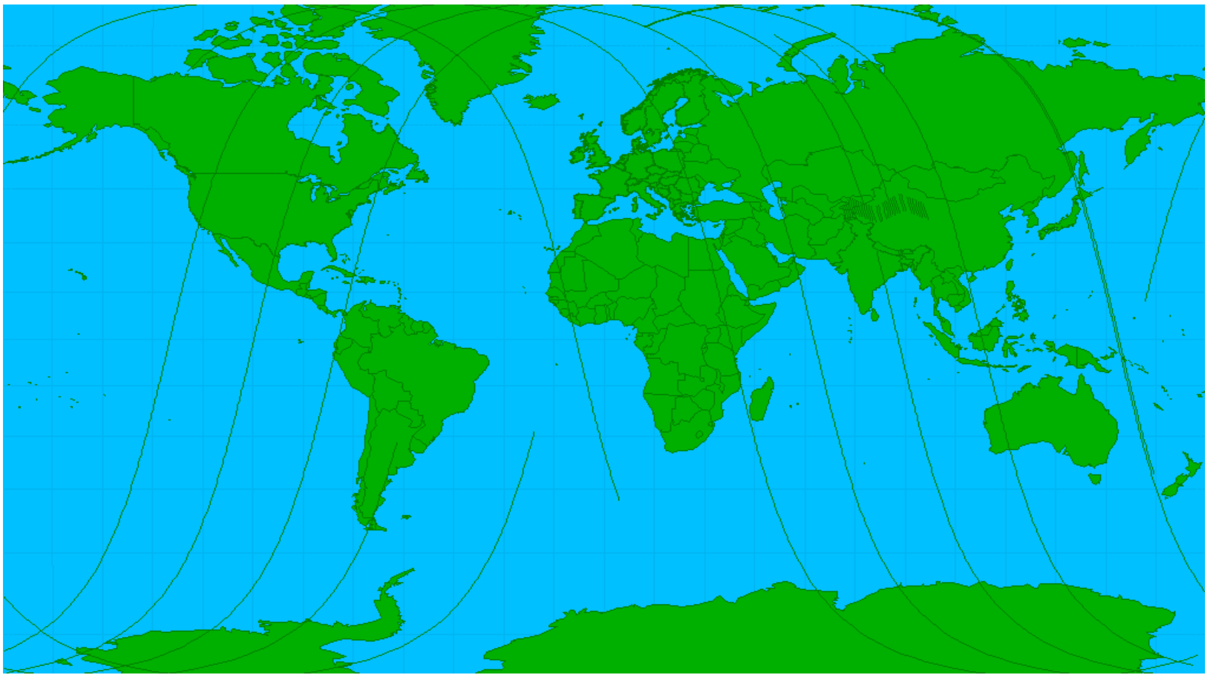

Figure 8: RA-2 L0 unavailable products for first part of cycle 28

Start date	Start time	Stop date	Stop time	Duration (s)	Start orbit	Stop orbit	Reason
22-giu-04	16.36.45	22-giu-04	16.38.03	78	12090	12090	PDS_UNKNOWN_FAILURE
23-giu-04	16.04.42	23-giu-04	16.06.00	78	12104	12104	PDS_UNKNOWN_FAILURE
24-giu-04	15.33.57	24-giu-04	15.35.15	78	12118	12118	PDS_UNKNOWN_FAILURE
25-giu-04	16.42.09	25-giu-04	16.43.27	78	12133	12133	PDS_UNKNOWN_FAILURE
26-giu-04	16.10.24	26-giu-04	16.11.42	78	12147	12147	PDS_UNKNOWN_FAILURE
27-giu-04	15.39.32	27-giu-04	15.40.50	78	12161	12161	PDS_UNKNOWN_FAILURE
28-giu-04	15.07.23	28-giu-04	15.08.41	78	12175	12175	PDS_UNKNOWN_FAILURE
29-giu-04	16.16.18	29-giu-04	16.17.36	78	12190	12190	PDS_UNKNOWN_FAILURE
30-giu-04	15.45.07	30-giu-04	15.46.25	78	12204	12204	PDS_UNKNOWN_FAILURE
01-lug-04	12.06.39	01-lug-04	12.09.06	147	12216	12216	PDS_UNKNOWN_FAILURE
01-lug-04	15.13.18	01-lug-04	15.14.36	78	12218	12218	PDS_UNKNOWN_FAILURE
02-lug-04	16.22.13	02-lug-04	16.23.31	78	12233	12233	PDS_UNKNOWN_FAILURE
03-lug-04	15.50.43	03-lug-04	15.52.01	78	12247	12247	PDS_UNKNOWN_FAILURE
04-lug-04	11.05.08	04-lug-04	12.14.07	4139	12258	12259	PDS_UNKNOWN_FAILURE
04-lug-04	15.19.13	04-lug-04	15.20.31	78	12261	12261	PDS_UNKNOWN_FAILURE
05-lug-04	16.28.09	05-lug-04	16.29.26	77	12276	12276	PDS_UNKNOWN_FAILURE
06-lug-04	15.56.19	06-lug-04	15.57.37	78	12290	12290	PDS_UNKNOWN_FAILURE
07-lug-04	15.25.09	07-lug-04	15.26.26	77	12304	12304	PDS_UNKNOWN_FAILURE
08-lug-04	16.34.03	08-lug-04	16.35.21	78	12319	12319	PDS_UNKNOWN_FAILURE
09-lug-04	15.59.26	09-lug-04	15.59.28	2	12333	12333	PDS_UNKNOWN_FAILURE
09-lug-04	16.01.55	09-lug-04	16.03.13	78	12333	12333	PDS_UNKNOWN_FAILURE
09-lug-04	22.20.28	09-lug-04	23.20.54	3626	12336	12337	PDS_UNKNOWN_FAILURE
10-lug-04	15.31.04	10-lug-04	15.32.22	78	12347	12347	PDS_UNKNOWN_FAILURE
11-lug-04	16.39.28	11-lug-04	16.40.46	78	12362	12362	PDS_UNKNOWN_FAILURE
14-lug-04	16.44.53	14-lug-04	16.46.11	78	12405	12405	PDS_UNKNOWN_FAILURE
15-lug-04	16.13.24	15-lug-04	16.14.41	77	12419	12419	PDS_UNKNOWN_FAILURE
16-lug-04	15.42.22	16-lug-04	15.43.40	78	12433	12433	PDS_UNKNOWN_FAILURE
17-lug-04	15.10.23	17-lug-04	15.11.41	78	12447	12447	PDS_UNKNOWN_FAILURE
18-lug-04	13.47.00	18-lug-04	13.47.03	3	12460	12460	PDS_UNKNOWN_FAILURE
18-lug-04	13.47.03	18-lug-04	16.16.44	8981	12460	12462	UNAV_RA2
18-lug-04	16.19.19	18-lug-04	19.59.00	13181	12462	12464	UNAV_RA2
18-lug-04	19.59.00	18-lug-04	20.00.05	65	12464	12464	PDS_UNKNOWN_FAILURE
19-lug-04	15.48.04	19-lug-04	15.59.32	688	12476	12476	PDS_UNKNOWN_FAILURE
20-lug-04	11.32.51	20-lug-04	12.11.57	2346	12487	12488	PDS_UNKNOWN_FAILURE
20-lug-04	15.13.59	20-lug-04	15.14.02	3	12490	12490	PDS_UNKNOWN_FAILURE
20-lug-04	15.16.18	20-lug-04	15.17.36	78	12490	12490	PDS_UNKNOWN_FAILURE
21-lug-04	16.25.13	21-lug-04	16.26.31	78	12505	12505	PDS_UNKNOWN_FAILURE
22-lug-04	15.50.50	22-lug-04	15.50.52	2	12519	12519	PDS_UNKNOWN_FAILURE
22-lug-04	15.53.33	22-lug-04	15.54.51	78	12519	12519	PDS_UNKNOWN_FAILURE
23-lug-04	15.19.37	23-lug-04	15.19.41	4	12533	12533	PDS_UNKNOWN_FAILURE
23-lug-04	15.22.13	23-lug-04	15.23.31	78	12533	12533	PDS_UNKNOWN_FAILURE

24-lug-04	16.31.08	24-lug-04	16.32.26	78	12548	12548	PDS_UNKNOWN_FAILURE
25-lug-04	15.59.09	25-lug-04	16.00.27	78	12562	12562	PDS_UNKNOWN_FAILURE

Table 5: List of gaps for RA-2 L0 products during cycle 28

In Figure 9 and Table 6 the summary of unavailable MWR L0 products is given.

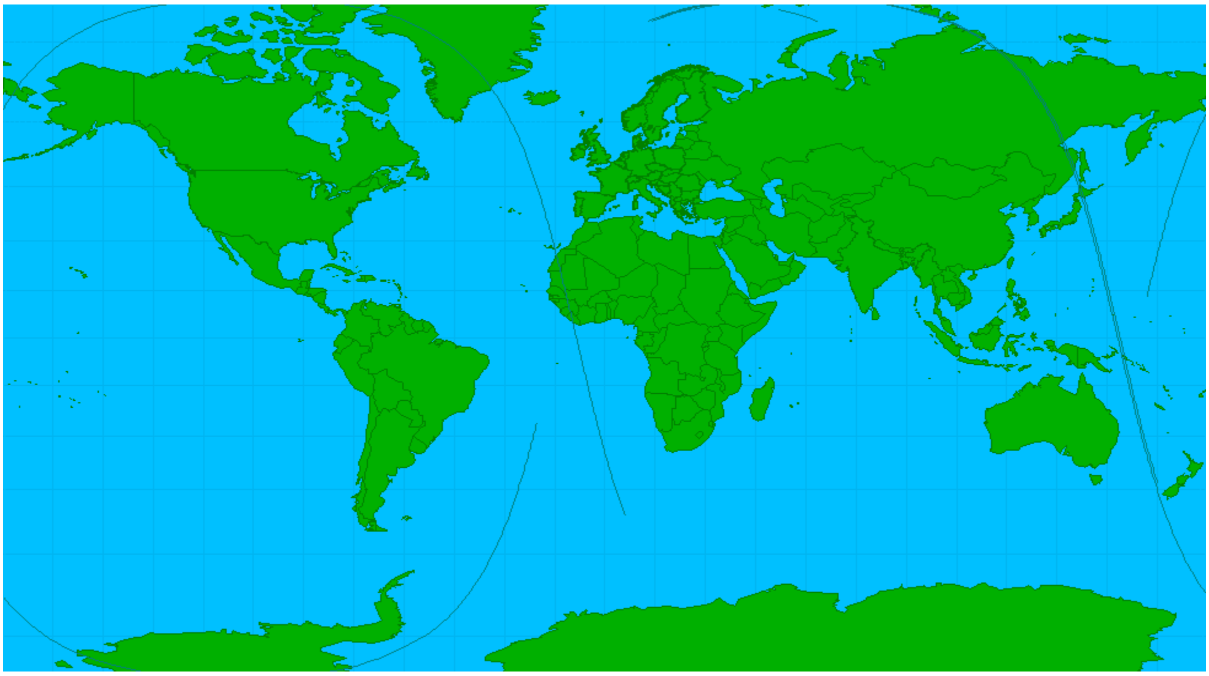

Figure 9: MWR L0 unavailable products for cycle 28

Start date	Start time	Stop date	Stop time	Duration (s)	Start orbit	Stop orbit	Reason
01-lug-04	12.05.57	01-lug-04	12.08.45	168	12216	12216	PDS_UNKNOWN_FAILURE
04-lug-04	11.04.28	04-lug-04	12.14.04	4176	12258	12259	PDS_UNKNOWN_FAILURE
04-lug-04	13.52.28	04-lug-04	13.53.16	48	12260	12260	PDS_UNKNOWN_FAILURE
08-lug-04	13.27.01	08-lug-04	13.27.49	48	12317	12317	PDS_UNKNOWN_FAILURE
09-lug-04	22.19.28	09-lug-04	23.20.40	3672	12336	12337	PDS_UNKNOWN_FAILURE
14-lug-04	11.58.50	14-lug-04	11.59.38	48	12402	12402	PDS_UNKNOWN_FAILURE
15-lug-04	14.45.17	15-lug-04	14.46.05	48	12418	12418	PDS_UNKNOWN_FAILURE
16-lug-04	12.35.43	16-lug-04	12.36.31	48	12431	12431	PDS_UNKNOWN_FAILURE
17-lug-04	12.05.21	17-lug-04	12.06.09	48	12445	12445	PDS_UNKNOWN_FAILURE
20-lug-04	11.32.15	20-lug-04	12.11.51	2376	12487	12488	PDS_UNKNOWN_FAILURE
21-lug-04	13.18.18	21-lug-04	13.19.06	48	12503	12503	PDS_UNKNOWN_FAILURE
22-lug-04	12.47.56	22-lug-04	12.48.44	48	12517	12517	PDS_UNKNOWN_FAILURE

Table 6: List of gaps for MWR L0 products during cycle 28

In Figure 10 and Table 7 the summary of unavailable RA-2 L1b products is given. Please note that in this case, only the gaps due to problems with the PDS are reported.

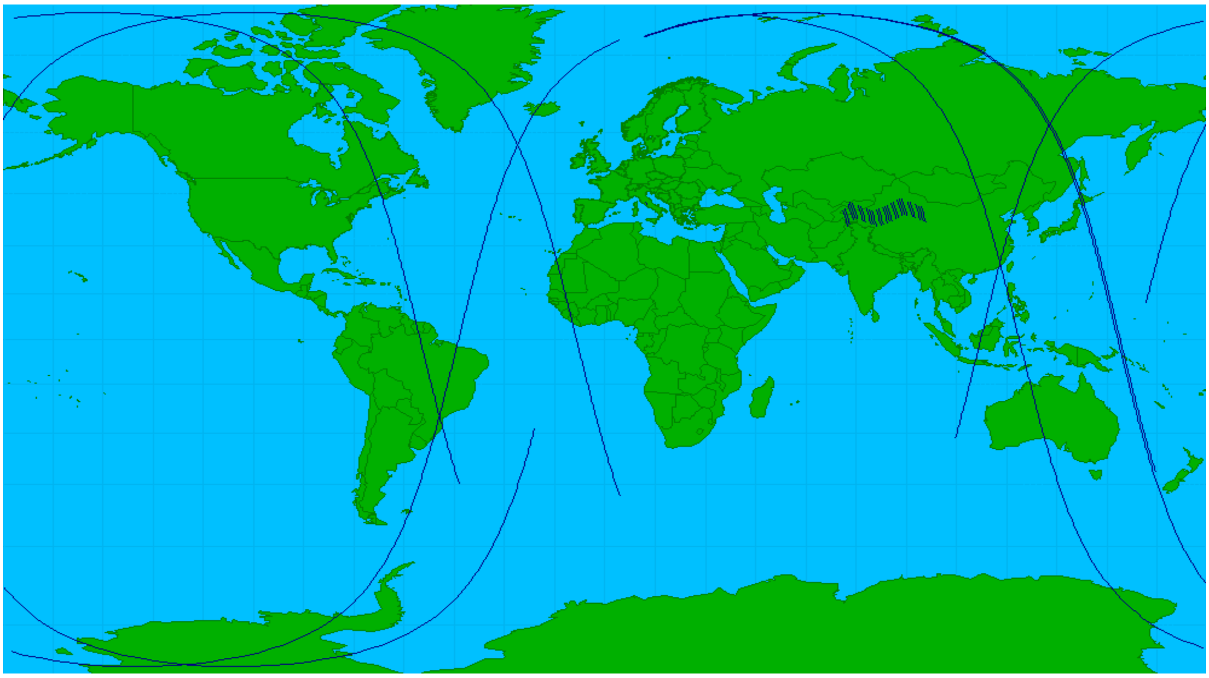

Figure 10: RA-2 L1b unavailable products for cycle 28

Start date	Start time	Stop date	Stop time	Duration (s)	Start orbit	Stop orbit	Reason
22-giu-04	16.36.45	22-giu-04	16.38.03	78	12090	12090	PDS_UNKNOWN_FAILURE
23-giu-04	16.04.42	23-giu-04	16.06.00	78	12104	12104	PDS_UNKNOWN_FAILURE
24-giu-04	15.33.57	24-giu-04	15.35.15	78	12118	12118	PDS_UNKNOWN_FAILURE
25-giu-04	16.42.09	25-giu-04	16.43.27	78	12133	12133	PDS_UNKNOWN_FAILURE
26-giu-04	16.10.24	26-giu-04	16.11.42	78	12147	12147	PDS_UNKNOWN_FAILURE
29-giu-04	16.16.18	29-giu-04	16.17.36	78	12190	12190	PDS_UNKNOWN_FAILURE
30-giu-04	15.45.07	30-giu-04	15.46.25	78	12204	12204	PDS_UNKNOWN_FAILURE
01-lug-04	12.06.40	01-lug-04	12.09.06	146	12216	12216	PDS_UNKNOWN_FAILURE
01-lug-04	15.13.18	01-lug-04	15.14.36	78	12218	12218	PDS_UNKNOWN_FAILURE
02-lug-04	16.22.13	02-lug-04	16.23.31	78	12233	12233	PDS_UNKNOWN_FAILURE
03-lug-04	15.50.43	03-lug-04	15.52.01	78	12247	12247	PDS_UNKNOWN_FAILURE
04-lug-04	11.05.09	04-lug-04	12.14.07	4138	12258	12259	PDS_UNKNOWN_FAILURE
06-lug-04	15.56.19	06-lug-04	15.57.37	78	12290	12290	PDS_UNKNOWN_FAILURE
07-lug-04	15.25.09	07-lug-04	15.26.26	77	12304	12304	PDS_UNKNOWN_FAILURE
08-lug-04	16.34.03	08-lug-04	16.35.21	78	12319	12319	PDS_UNKNOWN_FAILURE
09-lug-04	16.01.55	09-lug-04	16.03.13	78	12333	12333	PDS_UNKNOWN_FAILURE
09-lug-04	22.20.29	09-lug-04	23.20.54	3625	12336	12337	PDS_UNKNOWN_FAILURE
10-lug-04	15.31.04	10-lug-04	15.32.22	78	12347	12347	PDS_UNKNOWN_FAILURE
13-lug-04	12.32.16	13-lug-04	14.09.39	5843	12388	12389	PDS_UNKNOWN_FAILURE
13-lug-04	15.36.46	13-lug-04	15.38.04	78	12390	12390	PDS_UNKNOWN_FAILURE
13-lug-04	20.39.28	13-lug-04	20.39.43	15	12393	12393	PDS_UNKNOWN_FAILURE
14-lug-04	16.44.53	14-lug-04	16.46.11	78	12405	12405	PDS_UNKNOWN_FAILURE

15-lug-04	16.13.24	15-lug-04	16.14.41	77	12419	12419	PDS_UNKNOWN_FAILURE
16-lug-04	15.42.22	16-lug-04	15.43.40	78	12433	12433	PDS_UNKNOWN_FAILURE
17-lug-04	15.10.23	17-lug-04	15.11.41	78	12447	12447	PDS_UNKNOWN_FAILURE
18-lug-04	13.47.01	18-lug-04	13.47.03	2	12460	12460	PDS_UNKNOWN_FAILURE
20-lug-04	1.28.12	20-lug-04	2.40.04	4312	12481	12482	PDS_UNKNOWN_FAILURE
20-lug-04	11.32.41	20-lug-04	11.32.51	10	12487	12487	PDS_UNKNOWN_FAILURE
20-lug-04	11.32.51	20-lug-04	12.11.57	2346	12487	12488	PDS_UNKNOWN_FAILURE
20-lug-04	12.11.57	20-lug-04	12.11.58	1	12488	12488	PDS_UNKNOWN_FAILURE
20-lug-04	15.16.18	20-lug-04	15.17.36	78	12490	12490	PDS_UNKNOWN_FAILURE
21-lug-04	16.25.13	21-lug-04	16.26.31	78	12505	12505	PDS_UNKNOWN_FAILURE
22-lug-04	15.53.33	22-lug-04	15.54.51	78	12519	12519	PDS_UNKNOWN_FAILURE
23-lug-04	15.22.13	23-lug-04	15.23.31	78	12533	12533	PDS_UNKNOWN_FAILURE
24-lug-04	16.31.08	24-lug-04	16.32.26	78	12548	12548	PDS_UNKNOWN_FAILURE
25-lug-04	15.59.09	25-lug-04	16.00.27	78	12562	12562	PDS_UNKNOWN_FAILURE

Table 7: List of gaps for RA-2 L1b products during cycle 28

8.2 RA-2 Altimeter Parameters

Hereafter a summary of the main Altimetric parameters performances is reported; these results have been obtained with the editing criteria mentioned in par. 8.3.

8.2.1 ALTIMETER RANGE

No current results for the time being. The monitoring of the RA-2 FD altimetric range shall be done once the NRT products shall be upgraded with the DORIS navigator NRT orbital information.

8.2.2 SIGNIFICANT WAVE HEIGHT

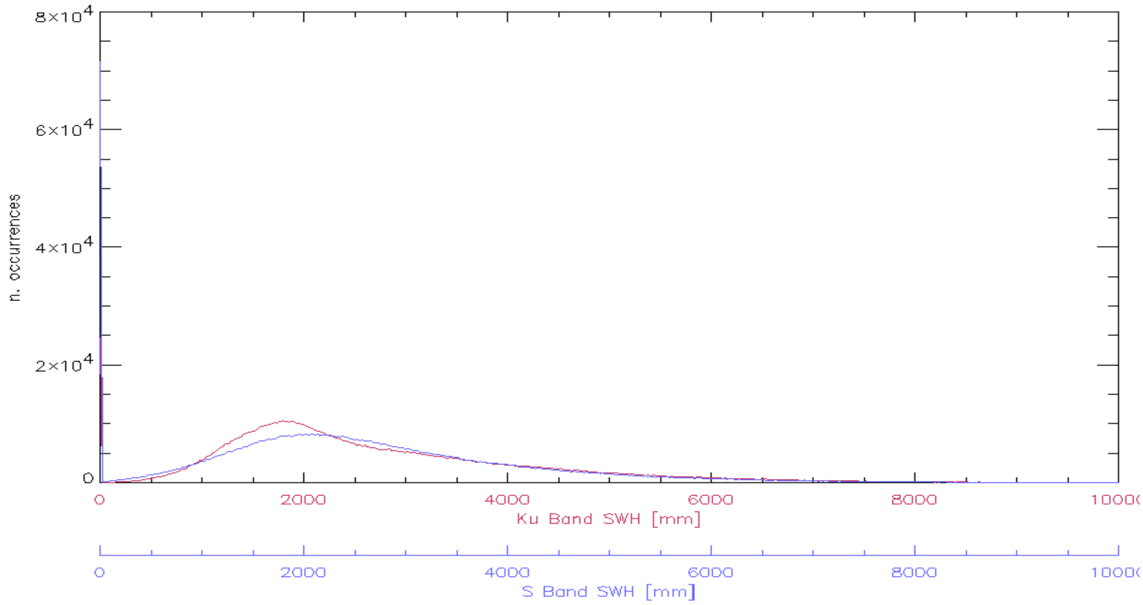

Figure 11: Histogram of Ku and S Band SWH for cycle 28 (mm)

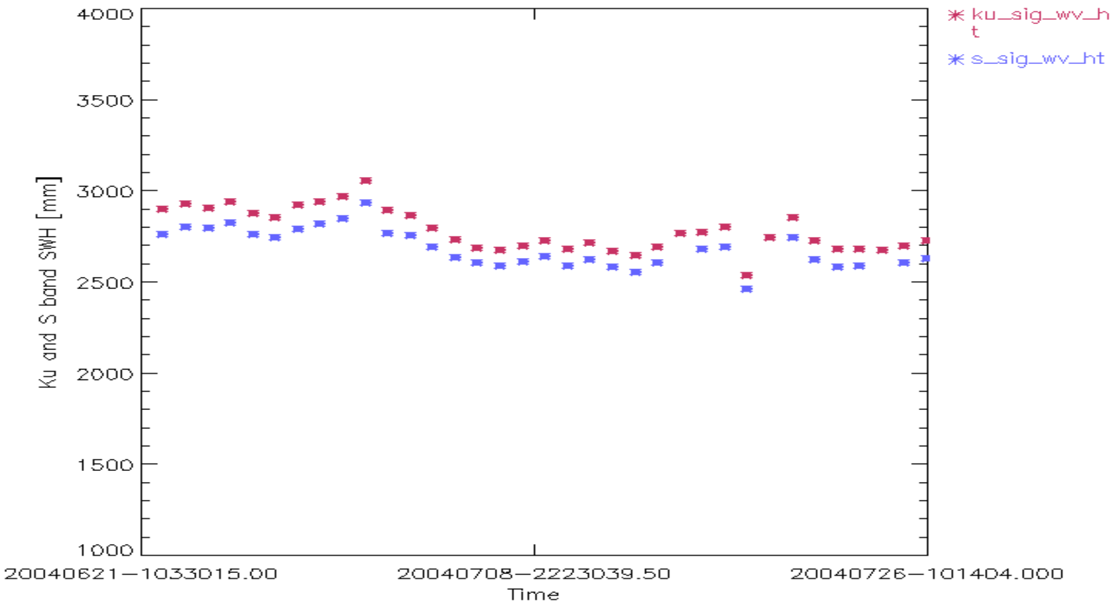

Figure 12: Ku and S SWH daily average for cycle 28 (mm)

The histogram of the SWH shows a nominal behavior for this cycle while for the trend a change in the behavior is detectable at the beginning of July. On July the 2nd the SWH value in the two bands drops of about 10 cm in average and also the ratio between the Ku and S Band value decreases. The reason of this behavior is not yet clear since an investigation on this issue has been just initiated.

The high daily means (sometimes plotted outside the figure range) reported for the S-Band values are due to the so-called S-Band anomaly (ref. par.7.1.7).

8.2.3 BACKSCATTER COEFFICIENT – WIND SPEED

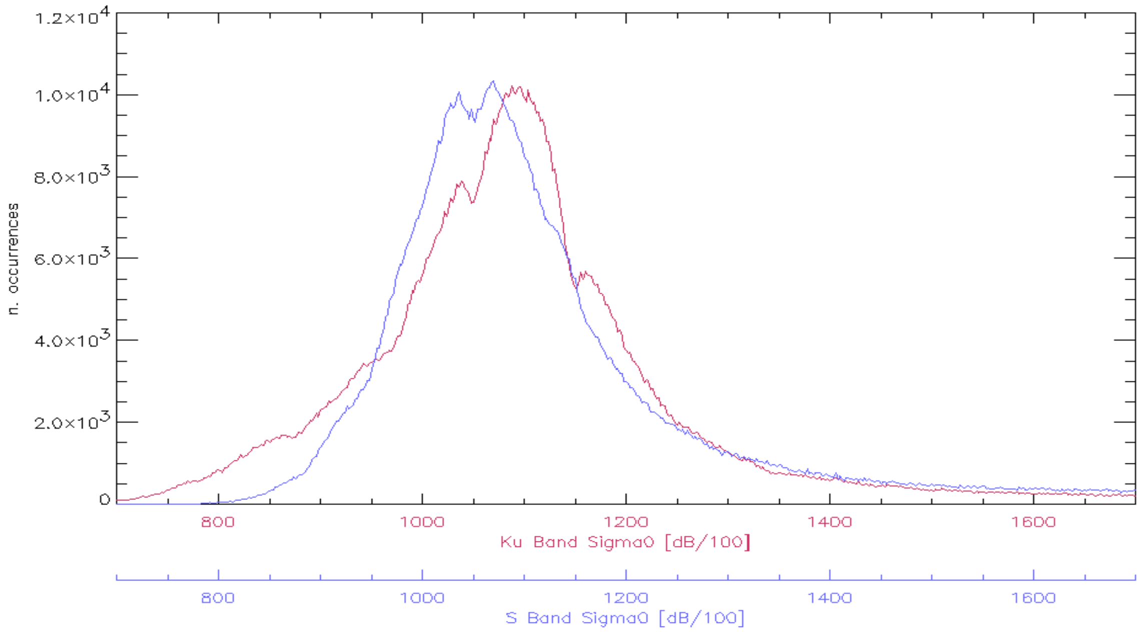

Figure 13: Histogram of Ku and S Band Backscattering Coefficient for cycle 28 (dB/100)

The Sigma_0 histogram both in Ku and S Band shows secondary peaks. A small investigation on this problem demonstrates that the backscattering distribution assumes a different behavior for different sea conditions. Indeed, for both the bands, the majority of the data is concentrated on lower values for rough sea state (southern hemisphere, winter conditions) and on higher values for calm sea state (northern hemisphere, summer conditions). This demonstrates that the instrument has a non-linear behavior respect to the backscattered power.

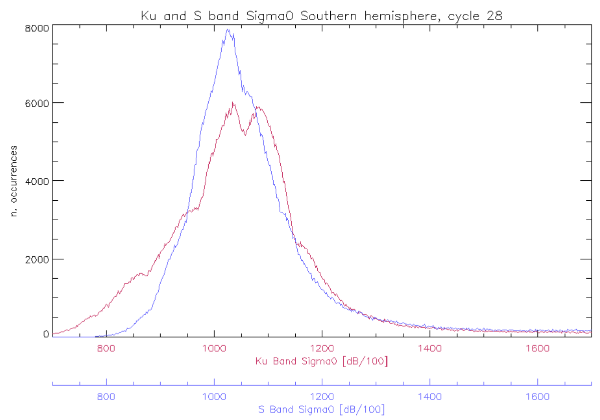

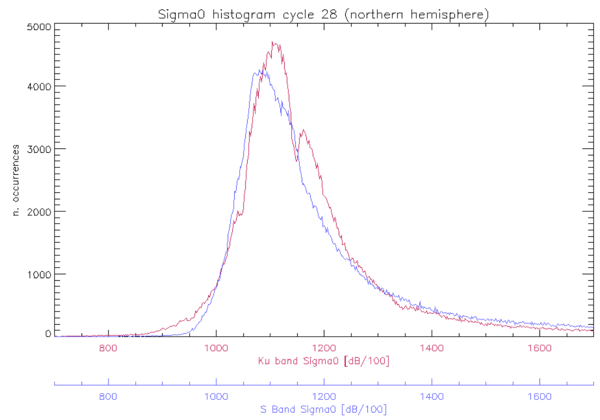

Figure 14: of Ku and S Band Backscattering Coefficient for cycle 28 (dB/100); southern hemisphere (left panel), northern hemisphere (right panel)

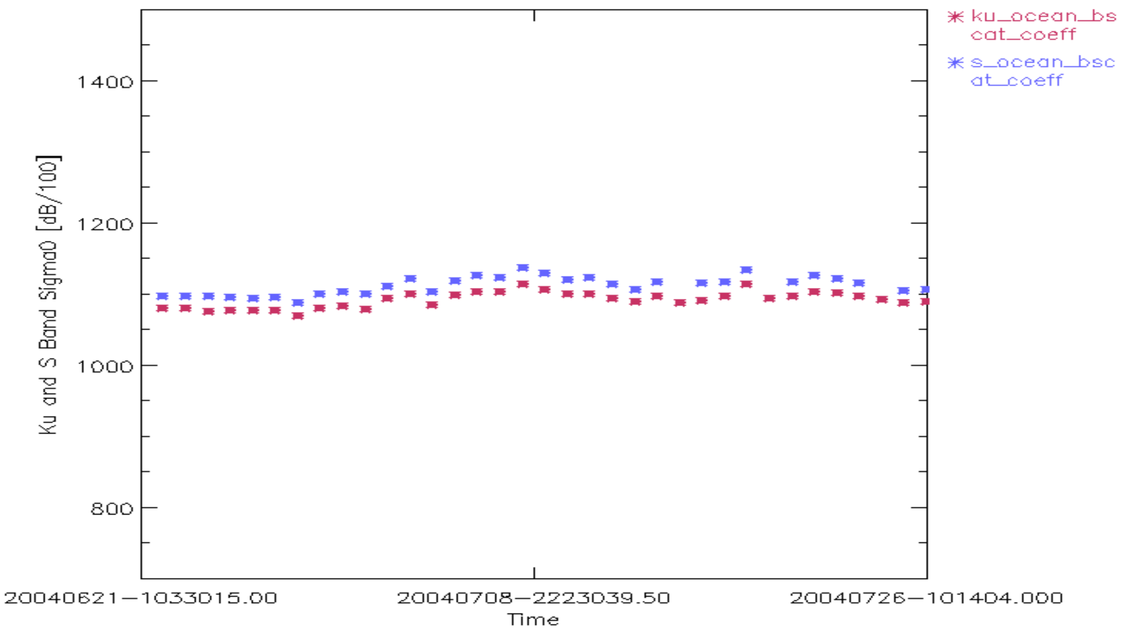

Figure 15: Ku and S Sigma_0 daily average for cycle 28 (dB/100)

The backscattering coefficient daily average trend shows, for both bands, a small increase of a tenth of a dB at the beginning of July 2004. This corresponds with the drop observed for the SWH, see Figure 12 and the reason behind this behavior is under investigation.

The high daily means (sometimes plotted outside the figure range) reported for the S-Band Sigma_0 trend are due to the so-called S-Band anomaly (ref. par. 7.1.7).

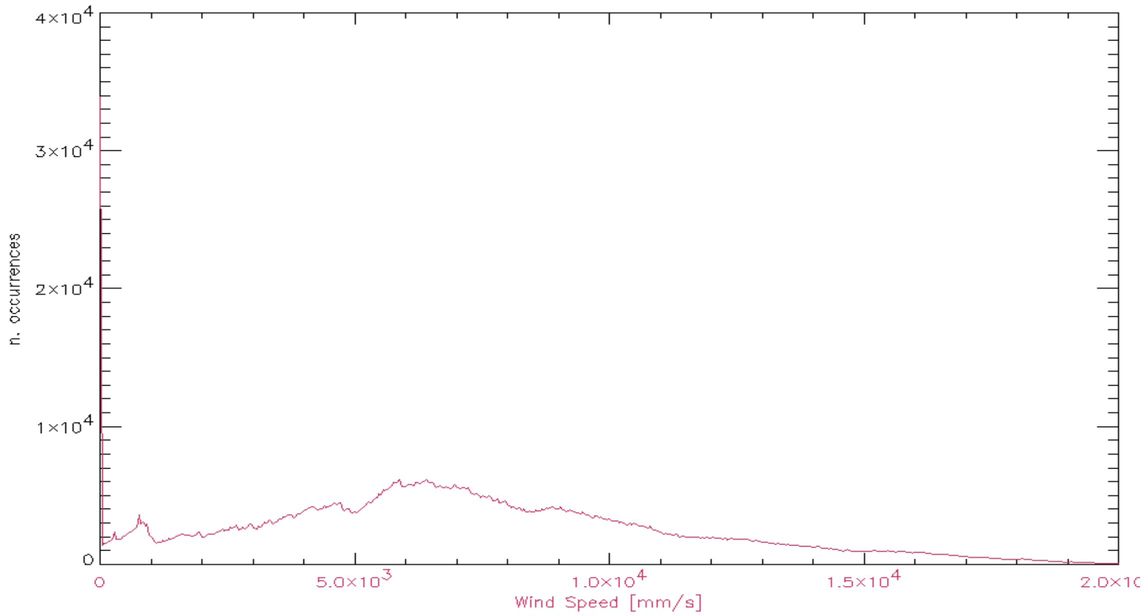

Figure 16: Histogram of Ku Wind Speed for cycle 28 (mm/s)

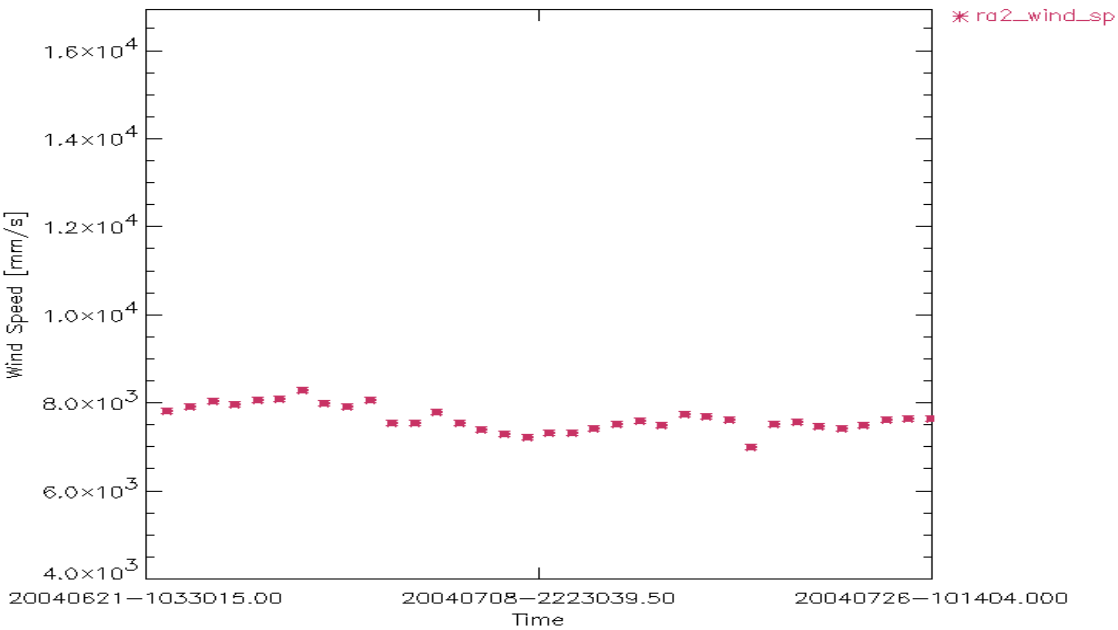

Figure 17: Wind Speed daily average for cycle 28 (mm/s)

8.3 Edited measurements

In order to produce the statistics reported in 8.2 the following editing criteria have been used before using RA2_FGD products:

Parameter	Surface type	Zone	Range
Ku SWH	Open Ocean	All world	[0, 10] (m)
Ku Backscattering Coeff.	Open ocean	All world	[7, 17] (dBs)
Ku Wind Speed	Open ocean	All world	[0, 20] (m/s)

Table 8: Editing criteria for RA-2 parameters statistics

8.4 Product disclaimer

For the product disclaimers please refer to the following web link:
http://envisat.esa.int/dataproducts/availability/

8.5 Data handling recommendations

8.5.1 SEA-ICE FLAG

The following algorithm is proposed for the determination of a sea-ice flag, presently missing in the Level 2 Ra-2 and MWR data products. (See [R – 14]):

|Latitude *(lat: field#4 of L2 data)*| >50 deg
AND
The number of 20Hz valid data *(num_18hz_ku_ocean: field#23 of L2 data)* < 17
OR
|MWR Wet Tropospheric Correction *(mwr_wet_tropo_corr: field#42 of L2 data)*–ECMWF Wet Tropospheric Correction *(mod_wet_tropo_corr: field#41 of L2 data)*| > 10 cm
OR
Peakiness *(Ku_peak: field#139 of L2 data)* >2

8.5.2 OCEAN S-BAND ANOMALIES DETECTION

A valuable algorithm to detect the Level 2 DSR affected by the RA-2 S-Band anomaly is proposed in [R- 12]. Note that its validity is limited to the data acquired over open-ocean.

8.5.3 WARNING ON IPF 4.56 VERSION IDENTIFICATION FIELD

All RA-2 and MWR level 1B and NRT Level 2 products generated after November 26, 2003 report a software version as being 4.54 (available in MPH field 8).

Nevertheless those products have been generated with the IPF V4.56 operational since November 26, 2003. The first nominal generated product, using the new SW version, will be the one relevant to the absolute orbit number 9094.

The software version ID is correct since December 4, 2003.

8.5.4 S-BAND BACKSCATTERING COEFFICIENT

For the data processed with IPF version 4.56 on, the S-Band Backscattering coefficient has been demonstrated to be in average about 0.65 dBs higher than for the previous versions of the processor. This is due to the algorithm used for the retrieval of the AGC in S-Band, corrected in IPF version 4.56 to be more coherent with the real functioning of the instrument.

An average value of 0.65 dBs is suggested to be added to the old software versions S-Band Sigma0 in order to be in line with the new IPF V4.56 version.

As a consequence of the IPF V4.56 s/w version installation, the rain flag validity is currently affected. This shall be corrected with the loading of a new ADF table.

8.5.5 USO RANGE CORRECTION

The actual data of cycle 28 have to be corrected to compensate for the Ultra Stable Oscillator drift shown in Figure 3. The measured Range shall be corrected considering a drift of –5.66 mm per year. Eventually it could also be corrected for the cyclic average given bias (28.59 mm) that has to be added to the measured value.

8.5.6 KU-BAND BACKSCATTERING COEFFICIENT CALIBRATION

The results of the Ku-Band Sigma0 absolute calibration performed with a transponder have been presented in par. 7.1.4. Those results are still not conclusive since some problems have still to be solved, in any case, in order to absolutely calibrate the backscattering coefficient given in the RA2 L2 products the following shall be used by the end user to get to the real Sigma0 measurement:

Sigma_0_true = Sigma_0_prod + **G_tx_rx_prod - G_tx_rx_real - Bias** [dB]

Where:
Bias: Bias retrieved from the Sigma0 Absolute Calibration
G_tx_rx_prod: Current effective Tx-Rx Gain value used in the operational ground processing chain (ADF file RA2_CHD_AX). The value nominally used since IPF V4.54 is (for configuration RFSS=A and HPA=A) is 170.70 dB
G_tx_rx_real: Pre-launch characterization value (configuration value RFSS=A and HPA=A is 167.46 dB)

8.6 Wind & Wave quality assessment

Refer to the ECMWF report given in [R – 9].

9 LONG TERM MONITORING

9.1 RA-2 Instrument monitoring

9.1.1 IF FILTER MASK

In Figure 18 the evolution of the IF mask quality parameters evaluated as in [R – 4] is reported only for valid data. It can be observed that the difference with respect to the on-ground reference stays quite constant around 0.07 dBs. Three peaks are visible on the plot that correspond to the data acquired on September the 27^{th} 2003 at 15:48, on October the 29^{th} 2003 at 15:42 and on May the 10^{th} 2004 at 15:45. The reason of this could be found in the instrument warming up considering that the IF Cal acquisition has been made, in all the cases, only a couple of hours after an anomaly recovery. The residual noise and the accuracy show a very constant behavior over the whole period.

Despite the quite constant IF mask trend, a weird behavior has been observed during the validation of several newly created IF mask correction auxiliary files. This phenomenon is currently under investigation but in the meantime the decision has been taken to avoid updating the auxiliary file in question.

During cycle 28 the IF Calibration Mode still shows the weird behavior described in [R – 3]. This problem, present since the beginning of the mission, is under investigation. The anomaly directly affects the number of valid RA-2 IF masks obtained per cycle, but does not refrain from the generation of the IF mask correction file, used in input to the Level 1 B ground processing.

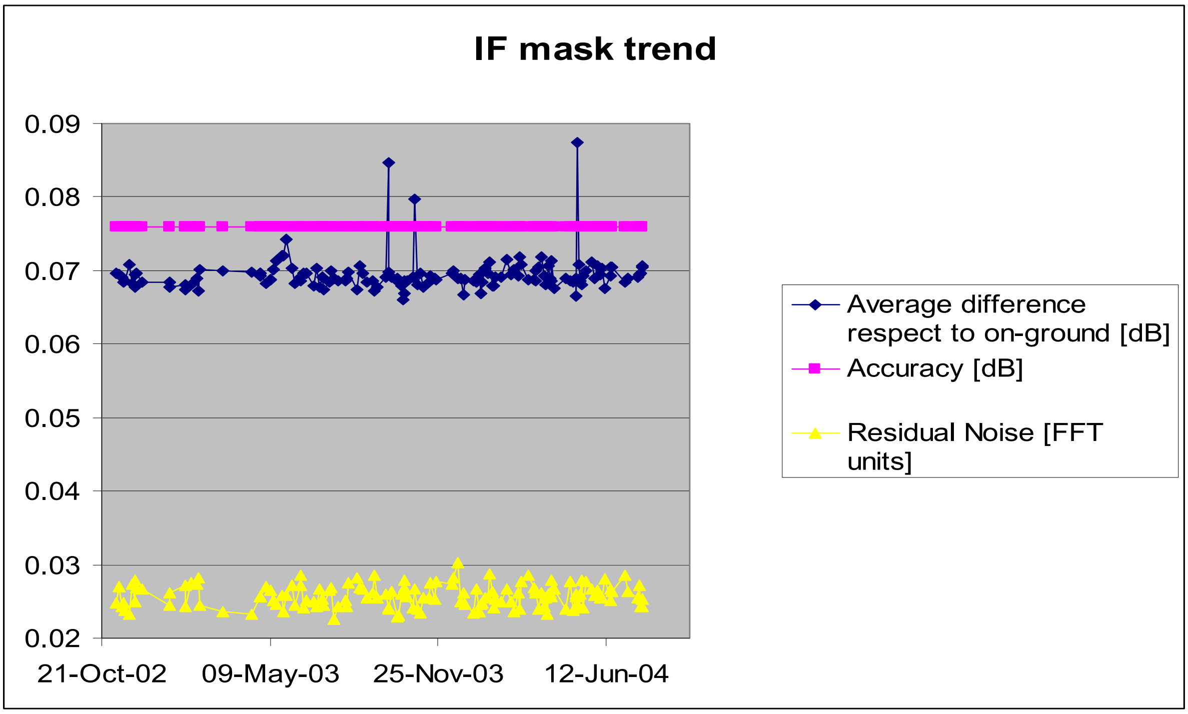

Figure 18: Evolution of the IF mask related parameters for valid IF masks retrieved up to cycle 28

9.1.2 USO

In Figure 19 the USO clock period trend retrieved until the end of cycle 28 is reported. In order to make the variability visible, the difference of the actual USO clock period with respect to the nominal one has been plotted, in the upper panel. In the lower panel the Range error due to the USO clock variability has been reported taking a satellite altitude of 800 Km as a nominal value.

Currently the nominal USO clock period (12500 ps) is used within the processing, this means that the data are not corrected for the bias and the drift correlated to the actual USO clock period. Those values, translated into altimetric range figures, are respectively of 32.29 mm and –3.82 mm/year as calculated with data covering the period 13 June 2003 to 27 July 2004. The given bias and drift have to be added to the original altimetric range.

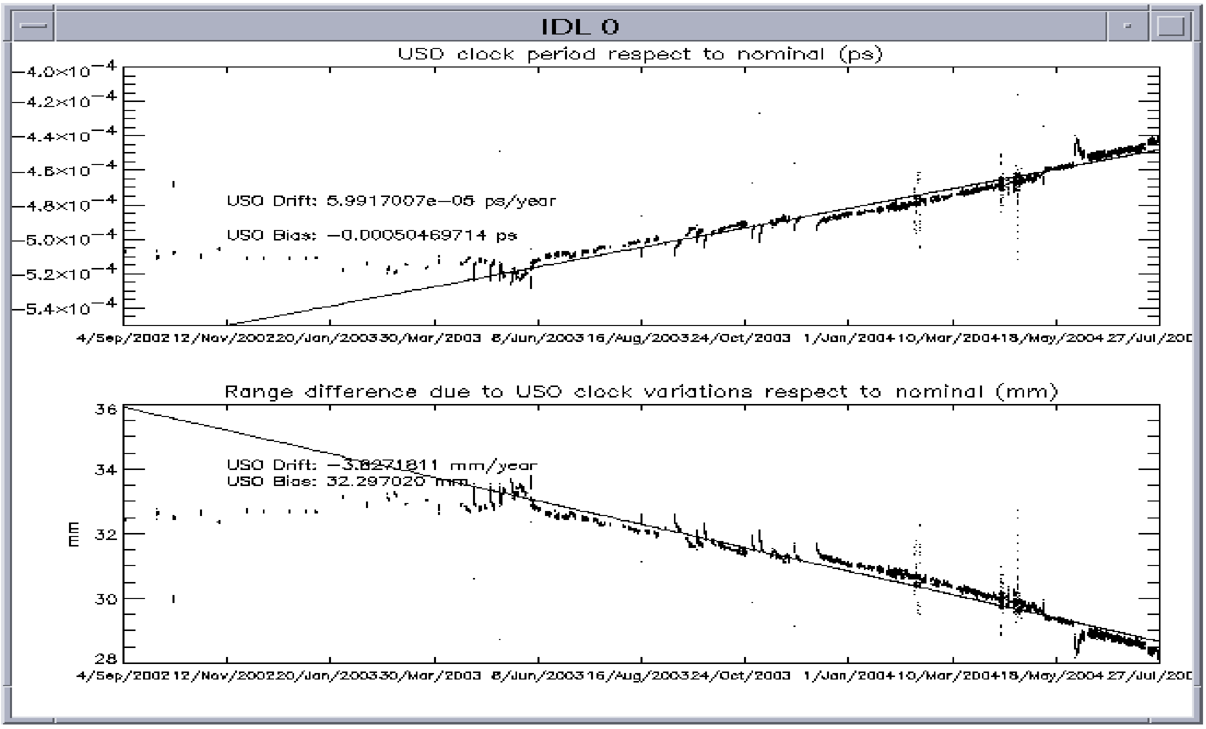

Figure 19: USO clock period until end of cycle 28

9.1.3 TRACKING CAPABILITY

In Figure 20, Figure 21 and Figure 22 the cyclic tracking percentages for the three RA-2 bandwidths are reported.
The worsening in performances noticeable for cycle 20 was due to the up-load of wrong on-board software parameters for the lasted for about three days.

In general, even if a tiny evolution can be observed, the tracking performances are well in line with the output figures and objectives of the Commissioning Phase as given in par. 7.1.3.

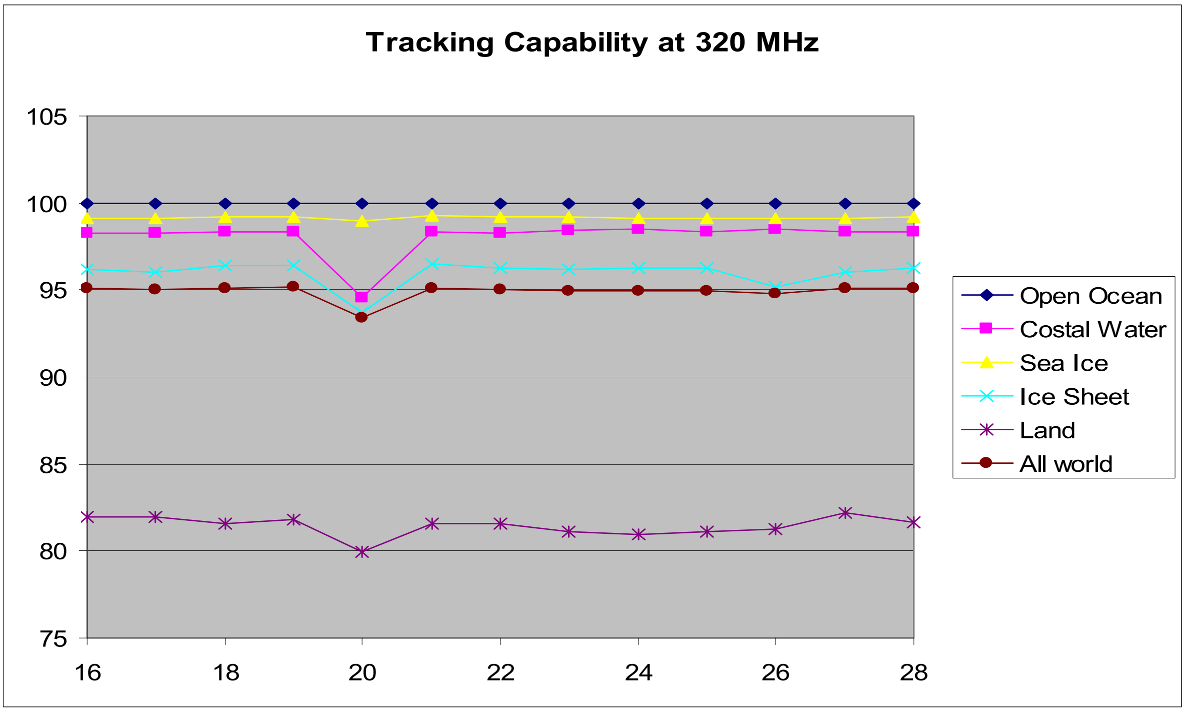

Figure 20: RA-2 Tracking percentage at 320MHz for different surfaces

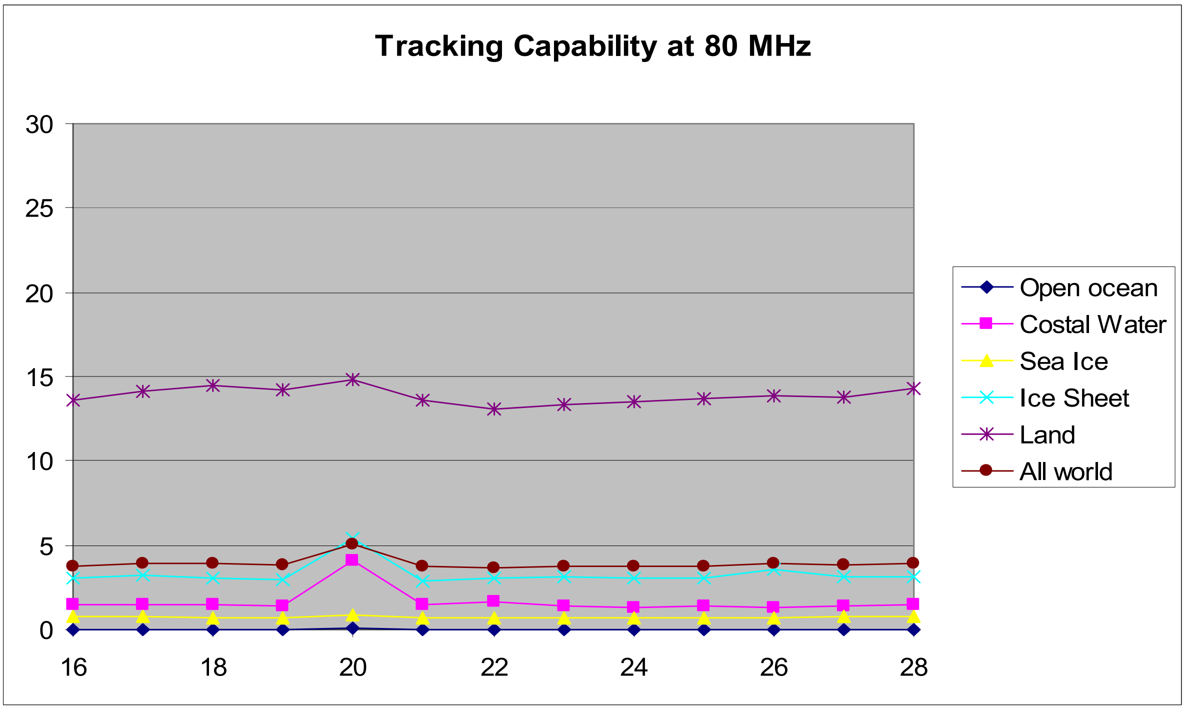

Figure 21: RA-2 Tracking percentage at 80MHz for different surfaces

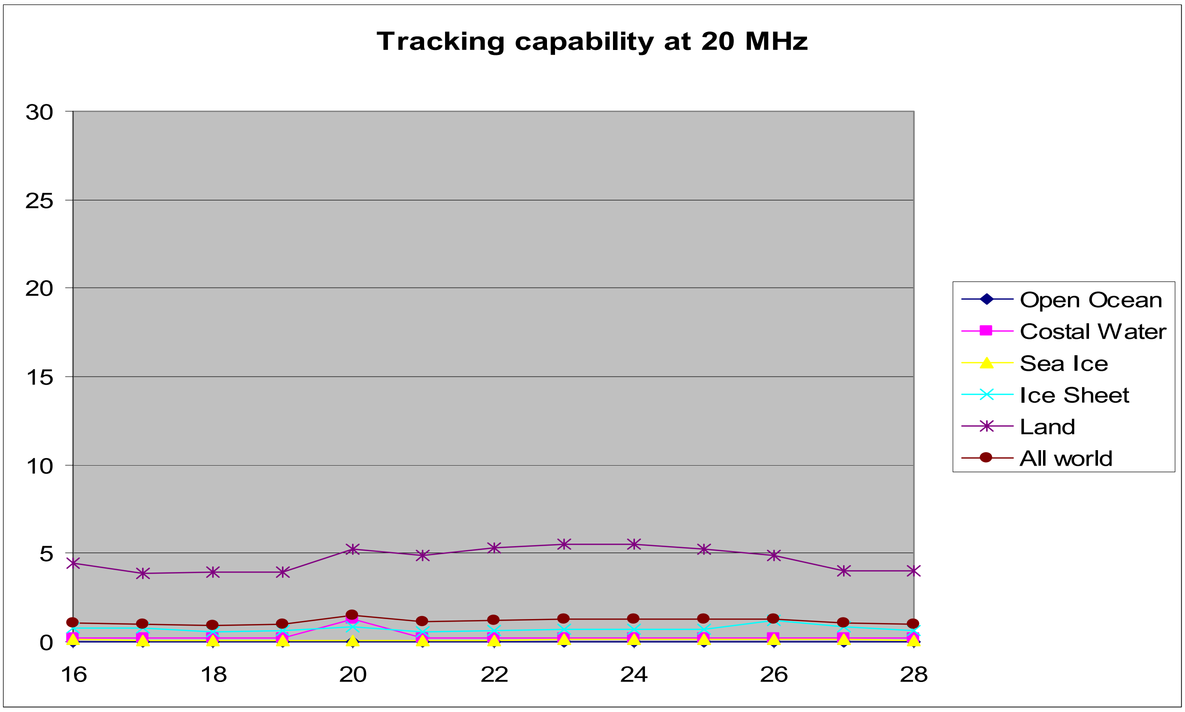

Figure 22: RA-2 Tracking percentage at 20MHz for different surfaces

9.1.4 DATATION

In Figure 23 (upper panel) the differences between the extrapolated UTC values and the corresponding real UTC values measured at the next Kiruna dump, are reported. Only few anomalous events can be observed at the beginning of the period (cycles 16/17) for which the difference rises above the 20 microseconds warning threshold. However, starting from cycles 22/23, the number of small differences (10 microseconds plus or minus) has increased a lot; this problem is currently under investigation.

In the lower panel the ICU clock step for the same period is shown where big variations are reported. This is however not a problem because the ICU clock period variations are included in the algorithm for the SBT/UTC correlation evaluation.

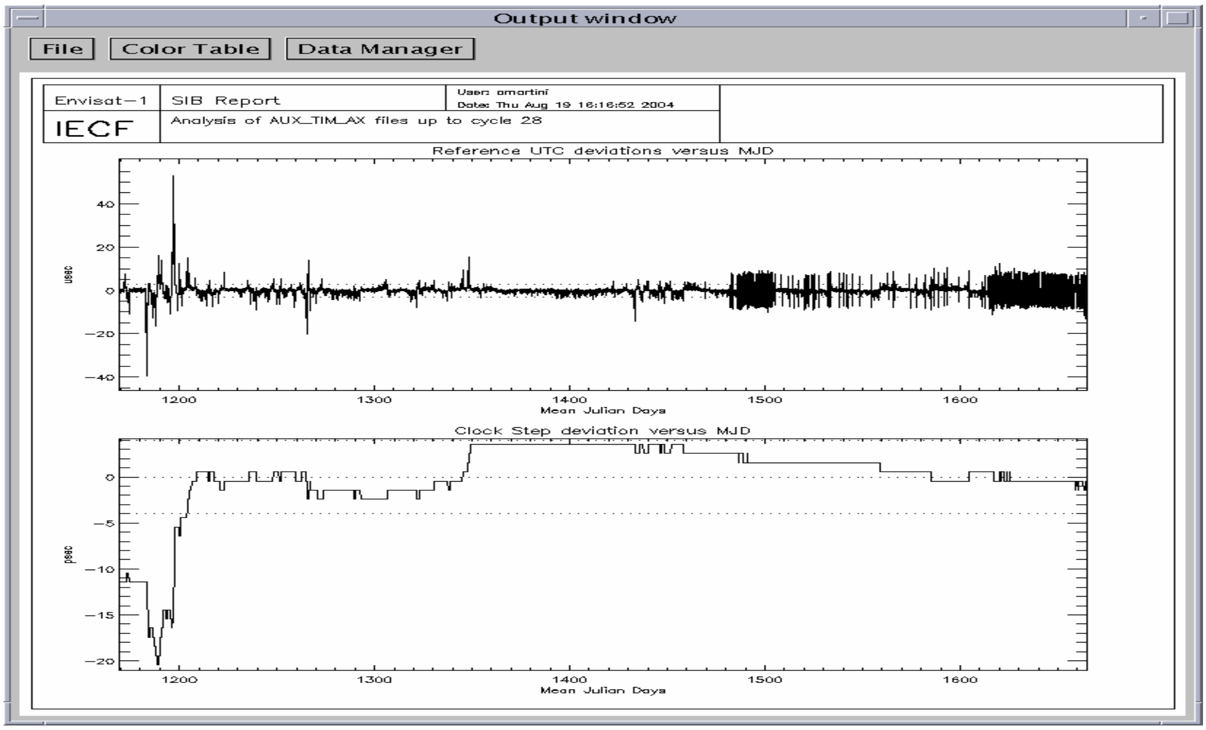

Figure 23: UTC deviations and ICU clock period up to cycle 28

9.1.5 MISPOINTING

In Figure 24 the overall mispointing squared trend (averaged over each orbit) is plotted for cycles 16 to 28. The jump occurred on November the 26th 2003 is correlated to the upload of IPF version 4.56; the abrupt decreasing of the mispointing squared value is due to the usage of a new RA2_IFF_AX IF mask auxiliary file.

On the other hand, it can be noticed that the mispointing squared assumes lower values just after an instrument anomaly; showing an increasing trend until it reaches back a standard mispointing value. This particular behavior can be explained by the different shape that the over-ocean average waveform has before and after an anomalous event as visible in Figure 25. Observe, in particular, the disappearance of the small dip in the waveforms acquired after the anomaly. This problem will be solved with the introduction of an updated mispointing retrieval algorithm with the next version of the processing software as described in par. 5.4.4.

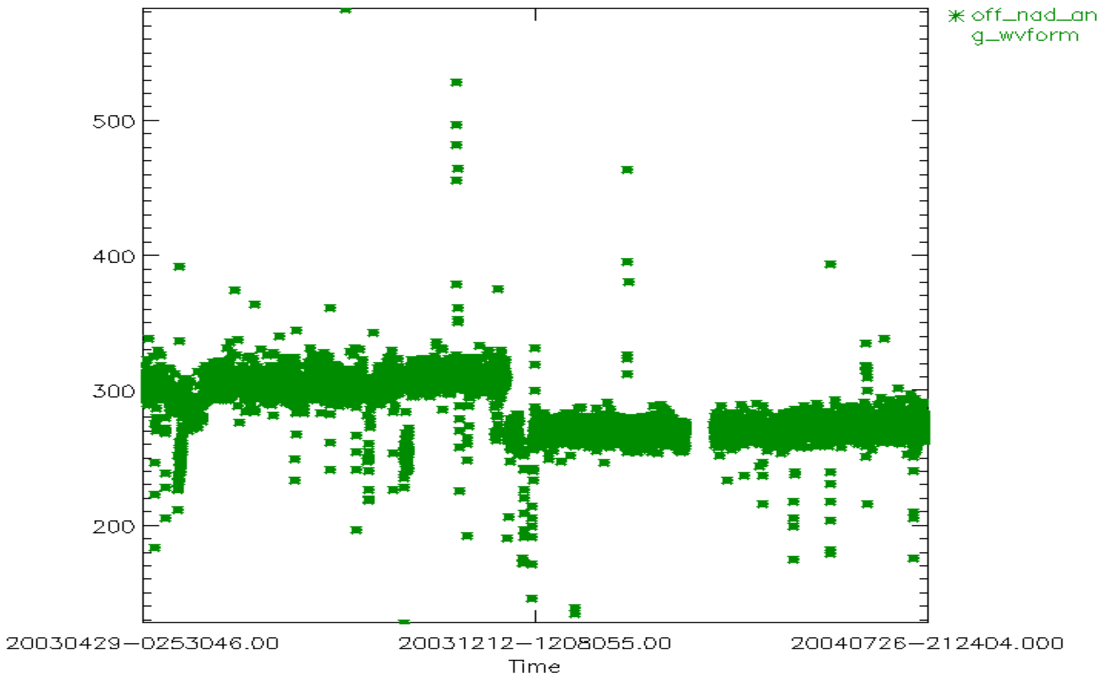

Figure 24: Smoothed mispointing squared trend until end of cycle 28 (deg^2*10e-4)

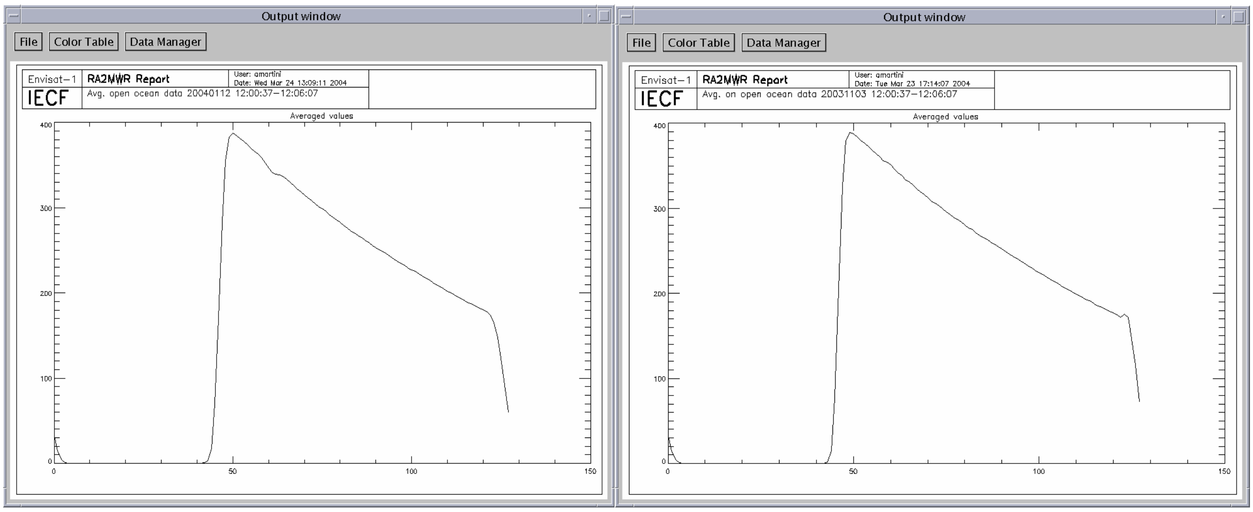

Figure 25: Open Ocean average waveforms before (left) and after an anomaly (right)

9.1.6 S-BAND ANOMALY

In the percentage of data per cycle that are affected by the so-called "S-Band" anomaly is reported. The figures are quite stable between 2.5% and 8.1%.
The relatively high value recorded for cycle 27 is due to the fact that on the day 1st of June, the S-band anomaly started at around 14:30 while the instrument didn't switch to mode Heater 2 when

foreseen (at about 15:50). For this reason the S-Band anomaly continued for the next 24 hours until the next Heater 2 mode on June the 2nd.

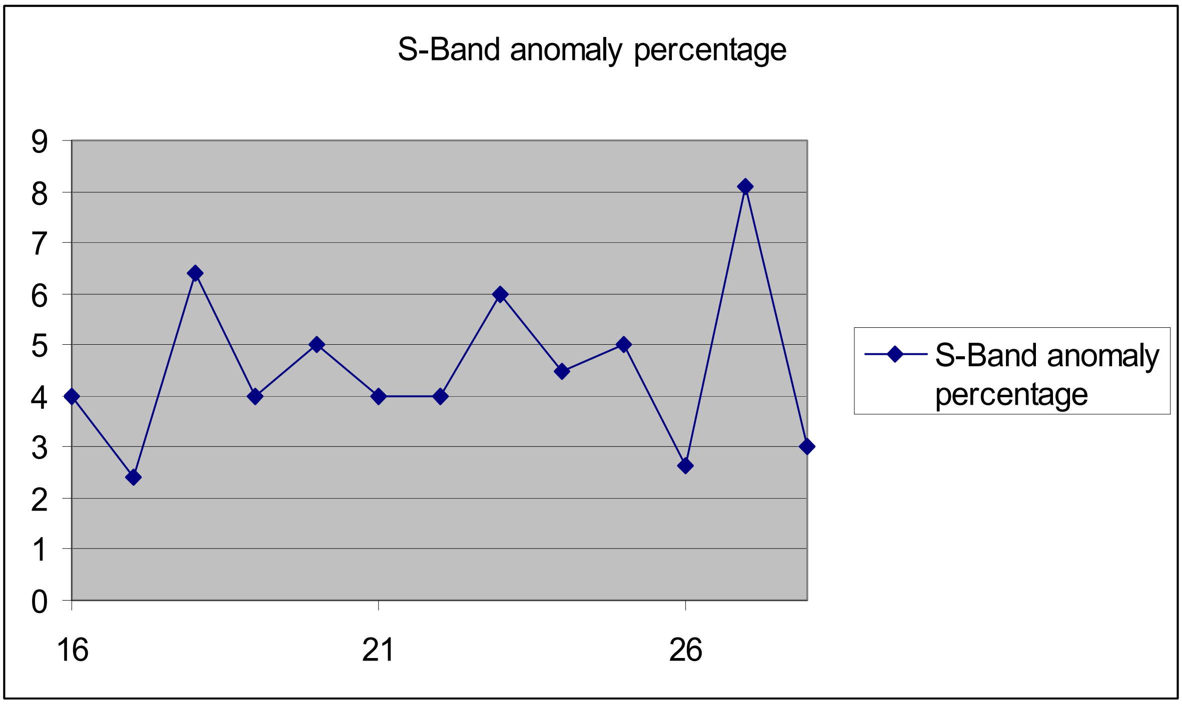

Figure 26: Percentage of data affected by the "S-Band Anomaly" for cycles 16-28

9.2 Products Monitoring

9.2.1 AVAILABILITY OF DATA

Hereafter the percentage of the different levels of products unavailability is reported for different cycles up to number 28. Considering as reference the instrument unavailability, it is possible to notice that in the last four months the situation is greatly improved for all levels of products.

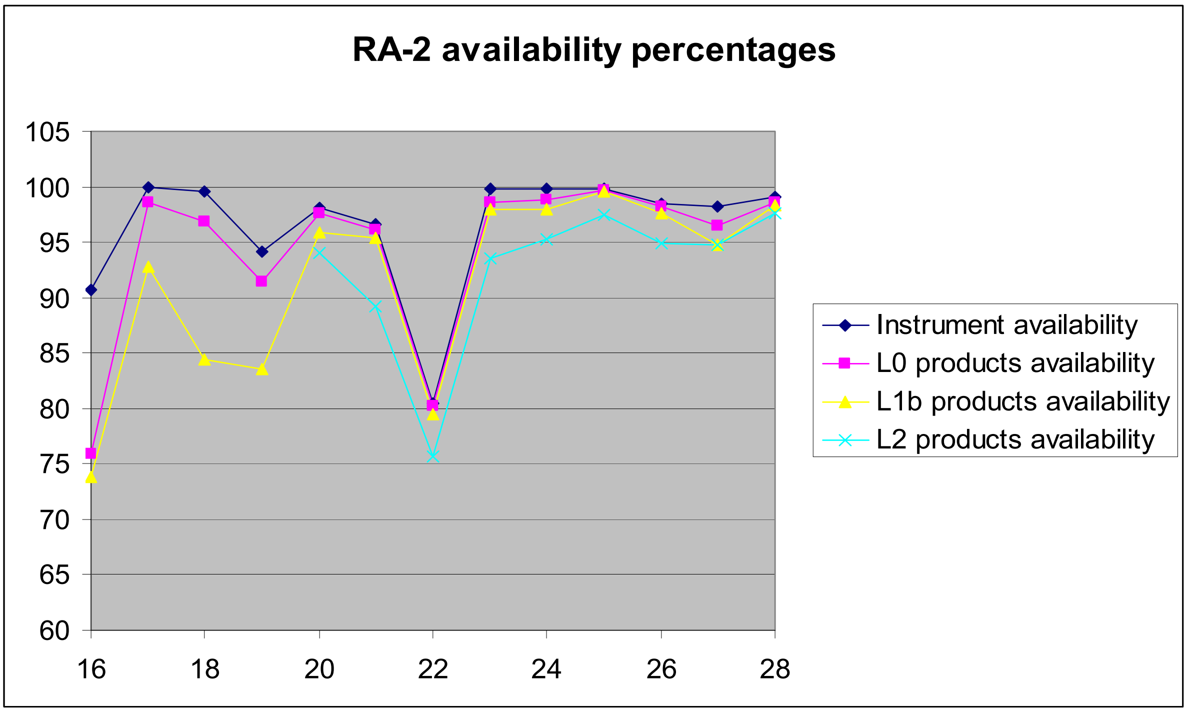

Figure 27: Percentage of Products unavailability up to cycle 28

9.2.2 RA-2 ALTIMETER PARAMETERS

Hereafter a summary of the main Altimetric parameters performances is reported; these results have been obtained with the editing criteria mentioned in par. 8.3.

9.2.2.1 Altimeter range

No current results for the time being. The monitoring of the RA-2 FD altimetric range shall be done once the NRT products shall be upgraded with the DORIS navigator NRT orbital information.

9.2.2.2 Significant Wave Height

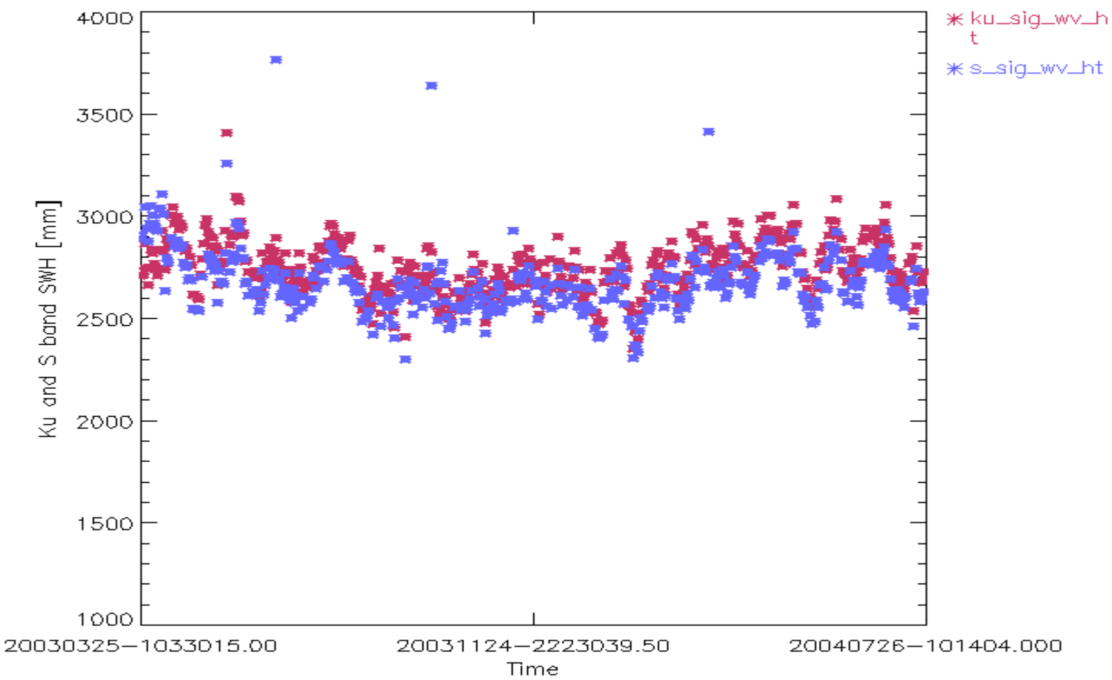

Figure 28: Ku and S SWH daily average up to cycle 28 (mm)

The SWH in both bands shows a small drop at the end of the time series which has been already mentioned in par. 8.2.2, this problem is currently under investigation. On the other hand, the S-Band SWH shows a drop on April the 9th 2003 corresponding to the operational up-load of IPF version 4.54; furthermore the high daily means reported (sometimes plotted outside the figure range) are due to the so-called S-Band anomaly (ref. par.7.1.7).

9.2.2.3 Backscatter coefficient – Wind Speed

The Ku-Band Sigma_0 trend, reported hereafter, is characterized by a jump of in average 3.24 dBs concomitant with the operational up-load of IPF version 4.54 occurred on the 9th of April 2004. To be said that this change is due to the upload of a new RA2_CHD_AX ADF file that artificially shifted the RA-2 real Sigma_0 in order to align it with ERS-2 Sigma_0 and make it coherent with the Witter and Chelton empirical wind model. A similar change in trend, but in the opposite direction, is also visible in the Wind Speed trend reported afterwards.

Beyond the huge jump occurred in April 2003, the S-Band Sigma_0 reports a smaller jump occurring on November the 26th 2003. Following the installation of the IPF processing chain V4.56, the average values of the RA-2 S-Band backscattering parameter, shows an increase of ~0.65 dBs, the new S-band sigma0 being higher with respect to the previous versions. See chapter 8.5.4.

During the last cycle another small increase of the backscattering coefficient in both Ku and S band has been recorded; the reason of this is currently under investigation as given in 8.2.3.

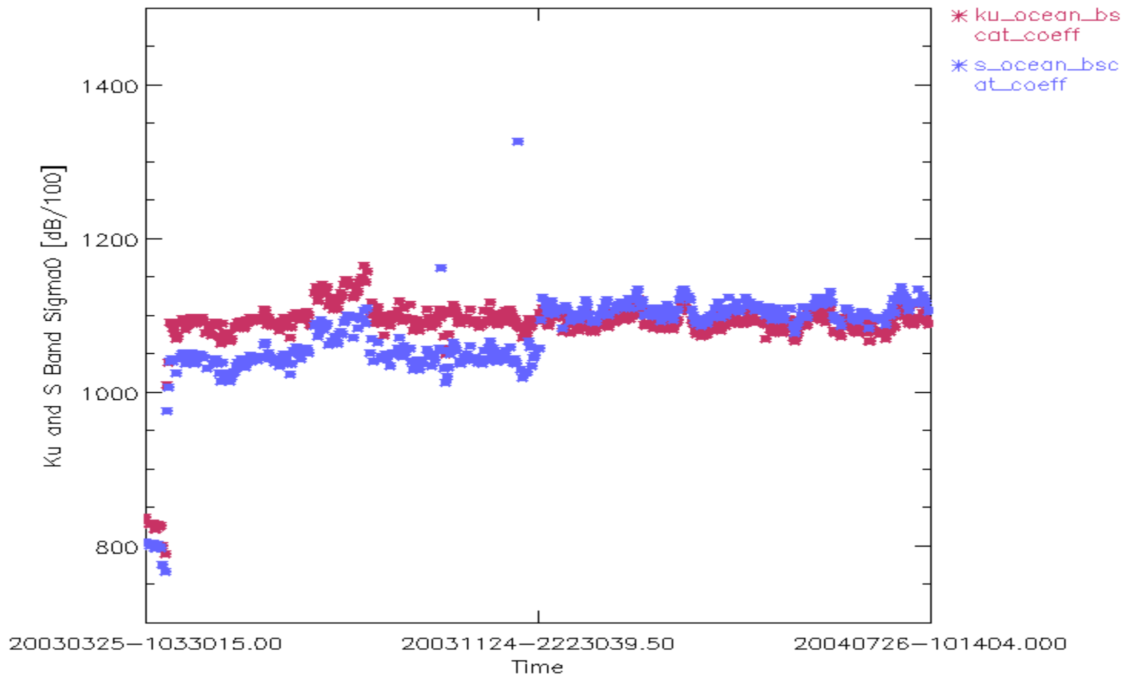

Figure 29: Ku and S Sigma_0 daily average up to cycle 28 (dB/100)

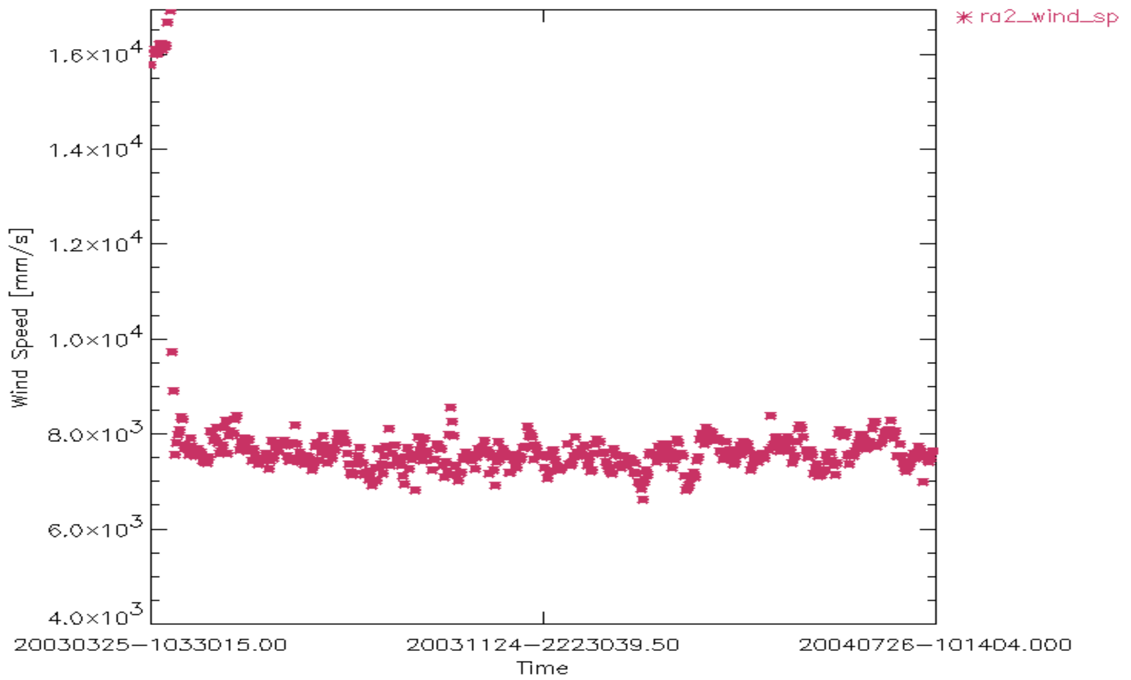

Figure 29: Wind Speed daily average for cycle 28 (mm/s)

10 PARTICULAR INVESTIGATIONS

During cycle 28 a special investigation has been performed in order to investigate the behavior of the backscattering histogram as reported in par 8.2.3.